Redox Biology 70 (2024) 103062

Contents lists available at ScienceDirect

Redox Biology

journal homepage: www.elsevier.com/locate/redox

VDR regulates mitochondrial function as a protective mechanism against renal tubular cell injury in diabetic rats

Hong Chen [a], Hao Zhang [a], Ai-mei Li [a], Yu-ting Liu [a], Yan Liu [a], Wei Zhang [a], Cheng Yang [a], Na Song [a], Ming Zhan [b], Shikun Yang [a,*]

[a] Department of Nephrology, The Third Xiangya Hospital, The Critical Kidney Disease Research Center, Central South University, China
[b] Department of Nephrology, The First Affiliated Hospital of Ningbo University, China

ARTICLE INFO

Keywords:
VDR
Mitochondrial
MAMs
DN
Renal tubular cell

ABSTRACT

Purpose: To investigate the regulatory effect and mechanism of Vitamin D receptor (VDR) on mitochondrial function in renal tubular epithelial cell under diabetic status.

Methods: The diabetic rats induced by streptozotocin (STZ) and HK-2 cells under high glocose(HG)/transforming growth factor beta (TGF-β) stimulation were used in this study. Calcitriol was administered for 24 weeks. Renal tubulointerstitial injury and some parameters of mitochondrial function including mitophagy, mitochondrial fission, mitochondrial ROS, mitochondrial membrane potential (MMP), mitochondrial ATP, Complex V activity and mitochondria-associated ER membranes (MAMs) integrity were examined. Additionally, paricalcitol, 3-MA (an autophagy inhibitor), VDR over-expression plasmid, VDR siRNA and Mfn2 siRNA were applied in vitro.

Results: The expression of VDR, Pink1, Parkin, Fundc1, LC3II, Atg5, Mfn2, Mfn1 in renal tubular cell of diabetic rats were decreased significantly. Calcitriol treatment reduced the levels of urinary albumin, serum creatinine and attenuated renal tubulointerstitial fibrosis in STZ induced diabetic rats. In addition, VDR agonist relieved mitophagy dysfunction, MAMs integrity, and inhibited mitochondrial fission, mitochondrial ROS. Co-immunoprecipitation analysis demonstrated that VDR interacted directly with Mfn2. Mitochondrial function including mitophagy, mitochondrial membrane potential (MMP), mitochondrial Ca^{2+}, mitochondrial ATP and Complex V activity were decreased dramatically in HK-2 cells under HG/TGF-β ambience. *In vitro* pretreatment of HK-2 cells with autophagy inhibitor 3-MA, VDR siRNA or Mfn2 siRNA negated the activating effects of paricalcitol on mitochondrial function. Pricalcitol and VDR over-expression plasmid activated Mfn2 and then partially restored the MAMs integrity. Additionally, VDR restored mitophagy was partially associated with MAMs integrity through Fundc1.

Conclusion: Activated VDR could contribute to restore mitophagy through Mfn2-MAMs-Fundc1 pathway in renal tubular cell. VDR could recover mitochondrial ATP, complex V activity and MAMs integrity, inhibit mitochondrial fission and mitochondrial ROS. It indicating that VDR agonists ameliorate renal tubulointerstitial fibrosis in diabetic rats partially via regulation of mitochondrial function.

1. Introduction

Diabetic nephropathy (DN) is a common serious complication of Diabetes mellitus (DM) [1], it is a main cause of end stage kidney disease in Western societies, with approximately 20 %–40 % of DM patients developing nephropathy. Traditionally, DN is dominated by glomerular involvement. Recently, studies have demonstrated that renal proximal tubular lesions plays an important role in the occurrence and development of DN [2,3], which has been defined as diabetic tubulopathy. A large number of studies suggested that the pathogenesis of DN included increased generation of reactive oxygen species (ROS), activation of renin-angiotensin system and infiltration of inflammatory cytokines.

* Corresponding author. Department of Nephrology The Third Xiangya Hospital, Central South University No.138, Tongzipo Road, Changsha, Hunan Province, 410013, China.

E-mail addresses: ch20165760806@163.com (H. Chen), zhanghaoliaoqing@163.com (H. Zhang), aimei_lam@163.com (A.-m. Li), 208311026@csu.edu.cn (Y.-t. Liu), 42730339@qq.com (Y. Liu), weizhangxy@126.com (W. Zhang), 727388097@qq.com (C. Yang), 875473635@qq.com (N. Song), stephen0726@163.com (M. Zhan), yangshikun@csu.edu.cn (S. Yang).

https://doi.org/10.1016/j.redox.2024.103062
Received 28 September 2023; Received in revised form 19 January 2024; Accepted 25 January 2024
Available online 26 January 2024

Regrettably, the most common hypoglycemic therapy using insulin or oral drugs could not completely prevent the progression of DN. The latest research indicated that mitochondrial dysfunction in renal tubular epithelial cell played a crucial pathogenic role in DN [4].

Vitamin D receptor (VDR) is a nuclear regulatory transcription factor. Mounting evidence suggested that vitamin D/VDR was involved in various renal diseases (e.g., DN) [5]. Conventional wisdom showed that the binding of vitamin D to VDR could repress or enhance the transcription of many genes through modification of the target gene promoter activity [6]. In addition to the nuclear effects of vitamin D/VDR, recently a new mitochondria regulatory mechanism of VDR has been suggested [7]. Emerging evidence showed that vitamin D/VDR had a far-reaching and effective regulatory effect on mitochondrial function and cell health in metabolic disorders [8]. Thus it was speculated that VDR-mitochondrial pathway might represent a promising therapeutic target for DN. Based on these above research, we completed this research to seek out the detailed effect and mechanism of VDR mediated mitochondrial function regulation in diabetes-induced renal tubular cell injury.

2. Research design and methods

Antibodies and reagents: Rabbit IgG antibody to VDR (#12550) and Rabbit IgG antibody to Drp1 (#8570) were purchased from Cell Signaling Technology (Massachusetts, USA). The fibronectin (FN) polyclonal antibody (15613-1-AP), Collagen type I (Col-1) monoclonal antibody (66761-1-Ig), LC3-specific polyclonal antibody (18725-1-AP), PINK1 polyclonal antibody (23274-1-AP), PARK2/Parkin monoclonal antibody (66674-1-Ig), ATG5 monoclonal antibody (66744-1-Ig) and FUNDC1 antibody (28519-1-AP) were purchased from Proteintech Group, Inc (Rosemont, USA). The mouse IgG antibody to sarcoendoplasmic reticulum Ca^{2+} ATPase 2 (SERCA2) (sc-376235) was obtained from SANTA CRUZ Biotechnology, Inc (Texas, USA). The rabbit IgG antibody to Mfn2 (12186-1-AP), anti-Mfn1(13798-1-AP), anti-Fis1 (10956-1-AP), anti-GAPDH antibody (10494-1-AP) and mouse IgG antibody to Cox IV (66110-1-Ig) and Mfn2 (67487-1-Ig) was obtained from Proteintech Group, Inc (Rosemont, USA). Other materials, including DMEM/F12 medium and bovine serum albumin (BSA) were obtained from GIBCO, ThermoFisher SCIENTIFIC (Massachusetts, USA), and fetal bovine serum was purchased from Procell Life Science&Technology (Wuhan, China). The recombinant human TGF beta 1 (TGF-β) protein (HZ-1011) was also purchased from Proteintech (Rosemont, USA). Streptozocin (STZ) was obtained from Sigma-Aldrich (St Louis. USA). The goat anti-rabbit IgG Alexa Fluor 488 (ab150077), the goat anti-mouse IgG Alexa Fluor 488 (ab150113), the goat anti-rabbit IgG Alexa Fluor 568 (ab175471) and the goat anti-mouse IgG Alexa Fluor 568 (ab175473) as fluorescent secondary antibodies were purchased from abcam (Cambridge, UK). The MitoTracker Red CMXRos (M7512) and MitoSOX Red (M36008) were purchased from Thermo Fisher Scientific (Massachusetts, USA). JC-1 kit (FS1166) was obtained from FUSHENBIO (Shanghai, China). ER-Tracker Blue (40761ES50) was purchased from Yeasen Biotechnology (Shanghai, China). Paricalcitol (S6681) and calcitriol (S1466) were obtained from Selleck Biotechnology (Texas, USA). 3-Methyladenine (3-MA, GC10710) was purchased from GlpBio Biotechnology (California, USA).

Animal experiment: A total of 18 eight-weeks-old male SD rats (~200 g B.W) were used in this study, they were obtained from HUNAN SJA Laboratory Animal Co,.LDT (Hunan, China), then the rats were divided randomly into 3 groups (6 rats in each group): Grouop 1 was a normal healthy control group. Group 2 was a diabetic model group. Group 3 was a calcitriol treatment group (calcitriol treated in a dose of 1ug/kg, orally/daily). The volume of calcitriol administrated was calculated so that each rat received a daily oral dose of 1ug/kg as reported [9,10]. Rats of group 2 and group 3 were intraperitoneal administration with STZ for four continuous days (40 mg/kg body weight each day) to establish a diabetic rat model as previously reported [11]. Then the blood glucose level of more than 16.7 mmol/l was considered as the standard for diabetic model. Moreover, the third group rats was administered calcitriol in fodder (1ug/kg). At the end of 24 weeks, all rats were killed to harvest the sera and kidney samples. The experimental procedure was approved by the Central South University Laboratory Animal Ethics Review Committee.

Renal morphological detection: Renal tissues were perfused with 4 % formaldehyde solution, after deparaffinization and rehydration, then the 4um slices of renal tissue were stained with Periodic acid-Schiff (PAS), hematoxylin-eosin (H&E) and Masson' s staining respectively. The assessment of renal tubulointerstitial injury in DN was carried out using a semiquantitative scoring system that was based on the established histopathological classification [12]. Specifically, a score of 0–3 was given based on the degree of interstitial fibrosis, tubular atrophy and interstitial inflammation. Similarly, glomerular injury was semiquantitative graded from 0 to 4 based on the degree of mesangial expansion, glomerular basement membrane thickening and glomerulosclerosis [12].

Serum biochemical index analysis: A blood glucose monitor (ROCHE ACCU-CHEK, Germany) was used to test the blood glucose every two weeks. 24 h urine of all rats was collected in individual metabolic cages, and then we used an rat albumin ELISA kit (EK-R37872, EK-Bioscience) to test urine albumin concentrations. In addition, the levels of serum creatinine (Scr), blood urea nitrogen (BUN), albumin (Alb) and calcium ion (Ca^{2+}) were measured using an automated biochemical analyzer (Hitachi 7600, Japan).

Immunofluorescence (IF) and immunohistochemistry (IHC) detection of renal tissue: Paraffin sections of rat kidney tissue were used for IF and IHC staining respectively. IF analysis of Col I and IHC analysis of LC3, PINK1, VDR and Mfn2 were performed as described previously [13]. Briefly, paraffin-embedded rat renal tissue sections (n = 6 rats per group, 3 μm thick) was prepared, after de-paraffinized, rehydrated and antigen retrieval, various first antibodies were incubated, then secondary antibodies conjugated with peroxidaseand was added. Finally, the diaminobenzidine (DAB) solution was added, and the section stained with brown color was defined as the sign of positive expression. Furthermore, various first antibodies and fluorescein labeled secondary antibody were used in the IF analysis. The optical densities of various index was calculated using Image J software (Version 1.53c, National Institutes of Health.USA).

Cell culture and intervention: The HK-2 proximal tubular epithelial cells of human were cultured at 37° Celsius in DMEM/F12 medium supplemented with 10 % fetal bovine serum. Previous study has confirmed that combination using TGF-β (10 ng/ml) and high glucose (30 mM) could effectively promote the production of extracellular matrix protein in HK-2 cells [14]. In order to induce a more significant profibrotic effect, high concentration of TGF-β(50 ng/ml) and high glucose (30 mM) stimulation were used to mimic diabetic renal tubular cell injury status in our study. Briefly, HK-2 cells were randomly divided into several groups: control group: D-glucose 5 mM, high glucose (30 mM) and TGF-β(50 ng/ml) intervention group, high glucose and TGF-βwith or without other interventions: paricalcitol (200 nM), 3-MA (5 mM) for indicated time (72 h) based on previous studies [15,16]. Furthermore, HK-2 cells were pretransfected with VDR overexpression plasmid, VDR siRNA or Mfn2 siRNA for gene disruption.

Gene intervention experiment: The construction of VDR overexpression-plasmid was carried out by Genechem (GeneChem Co. Ltd.,Shanghai, China).The full length VDR sequence was cloned into a GV146 expression vector. The full length VDR gene was obtained using the VDR primer 1: (5′-TACCGGACTCAGATCTCGAGCGCCACCATGGAGGCAATGGCGGCCAG-3′) and primer 2: (5′-TACCGTCGACTGCAGAATTCTCAAGGGACCGGGGAAAAGCCCG-3′). Human VDR small interfering RNA (siRNA) and Mfn2 siRNA were constructed by Guangzhou RIBOBIO CO., LTD. The Mfn2 siRNAs targeted the following sequences: Mfn2 A (5′-GGCCAAACATCTTCATCCT-3′), Mfn2 B (5′-CGGTTCGACTCATCATGGA-3′), and Mfn2 C (5′-

GCGAGGAAATGCGTGAAGA-3′). The VDR siRNAs targeted the following sequences: VDR A (5′-AGCGCATCATTGCCATACT-3′), VDR B (5′-GTCAGTTACAGCATCCAAA-3′), VDR C (5′-CCCACCATAA-GACCTACGA-3′). The sequences of negative control (referred to as siRNA control) was not been reported. The transfection of VDR-overexpression plasmid, Mfn2 siRNA or VDR siRNA were performed using Lipofectamine 3000 as previously reported [17]. Briefly, HK-2 cells were cultured in 6-well tissue culture plates and maintained in DMEM/F12 supplemented with 10 % FBS for 24 h until they reached 50 %–70 % confluence. Then, the cells were transfected with the VDR plasmid, VDR siRNA or Mfn2 siRNA using Lipofectamine 3000 reagent (Invitrogen, USA), and the empty plasmid was used as control. All experiments were performed in triplicate.

Western blotting experiment: The protein of renal tissue and HK-2 cells was isolated. Then protein was transferred onto a polyvinylidene difluoride membrane (Millipore, IPVH00010). The membranes were blocked with PBST containing 5 % nonfat milk for 1 h.Subsequently, these membranes were subjected to incubation with primary antibodies against FN, Col-1 (1:500), PINK1, Parkin, Atg5, Fundc1, LC3, Mfn2, Mfn1, Drp1,VDR, Fis1, SERCA2, GAPDH and Cox IV (1:1000) overnight at a temperature of 4 °C. After incubated with secondary antibody for 1 h, the membranes were visualized using an enhanced chemiluminiscent (ECL) system (Amersham, USA) following the manufacturer's instructions and previous reports [18]. Finally, Image J analysis software (Version 1.53c, National Institutes of Health.USA) was used for the quantitative analyzed of band density. All experiments were independently repeated for three times.

Co-immunoprecipitation analysis: The Co-immunoprecipitation kit (P2179 M) were obtained from Beyotime Biotechnology (Shanghai, China).The interaction between VDR and Mfn1, Mfn2, Drp1,Fis1 was detected by co-immunoprecipitation (CO-IP) as previously described [19]. Briefly, the cell protein was extracted using lysis buffer, the protein lysates were subject to immunoprecipitation with VDR antibody. Then protein G magnetic beads were used to immunoprecipitate, and a magnetic separator was used to isolate the supernatant. Finally, the immunoprecipitate was used to Western blot analysis. In addition, CO-IP analysis was performed to detect the interaction between Mfn2 and SERCA2.

Cells Immunofluorescence (IF) examination: After various treatments in vitro studies, HK-2 cells were first immersed in MitoTracker Red (1:1000) solution, then the cells were incubated with primary antibody against VDR (1:100 dilution) or LC3II (1:100 dilution) solution for 2 h at 22 °C. The cells were then incubated with secondary fluorescent antibody (combined using goat anti-rabbit IgG Alexa Fluor 488 and goat anti-mouse IgG Alexa Fluor 568, or goat anti-rabbit IgG Alexa Fluor 568 and goat anti-mouse IgG Alexa Fluor 488), and then DAPI solution. A confocal laser scanning microscope was used to detect cells fluorescence density, finally we calculated the relative fluorescence density of VDR, LC3II. For another, double IF staining of the ER and mitochondria was performed to observe the images of MAMs. Live HK-2 cells were incubated with ER blue (1:1000) and MitoTracker Red (1:1000) solution. The colocalization correlation analysis was performed using Image J colocalization finder (Version 1.53c, National Institutes of Health. USA) as previously reported [20].

Confocal microscopy observation: To carry out the confocal microscopy examination, we used a Zeiss LSM 780 META laser scanning microscope [21]. Briefly, after stained with various probes or fluorescent antibodies, HK-2 cells were prepared to confocal microscopy detection. Applications of confocal microscopy in our study included the imaging of multiple labeled specimens and the measurement of physiological events in either fixed or living cells. The Image J software (Version 1.53c, National Institutes of Health.USA) was used for images analysis.

Electron microscopy observation: The transmission electron microscopy (TEM) technique was employed to observe the morphology of mitochondria and the junctions between mitochondria and endoplasmic reticulum (ER) in both renal tissues and HK-2 cells. Samples for TEM detection were prepared as previously reported [22]. Briefly, 1 mm^3 pieces of fresh renal cortices was prepared, and then 60–80 nm ultrathin sections was cutted for further examination. On the other side, HK-2 cells were detached and washed with PBS solution, then glutaraldehyde and osmium tetroxide solution were used to fix cells. Observations were made using TEM to delineate the mitochondrial morphology and the ER-mitochondria contacts as previously reported [23].

Cell viability and proliferation detection: The cell viability was analyzed using a cell counting kit-8 assay (CCK-8, Beyotime, Nantong, China, C0037) as previously reported [24]. HK-2 cells were cultured in a 96-well plate, then different concentrations of TGF-β (10, 50 and 100 ng/ml) and high glucose (30 mM) were added for 24–72 h. After that, diluted CCK8 solution (100 μL/each well) were added to each well. Finally, a microplate reader was used to measure the optical density (OD) of each well at 450 nm.

Mitochondrial ROS and mitochondrial membrane voltage potential (MMP) detection: HK-2 cells from various experimental groups was prepared for further detection. Mitochondrial ROS was measured using a MitoSOX fluorescent

probe, as described before [25]. Cells were placed in confocal observation dishes. Following different experimental interventions, cells were treated with MitoSOX red probe (500 nmol/L) for 10 min at 37 °C. The cells were then washed twice with PBS, and the red fluorescence was determined using confocal microscopy. On the other side, the detection of MMP levels was conducted using the JC-1 probe, as previously explained [26]. In normal mitochondria, JC-1 aggregated in the mitochondrial matrix and emitted a robust red fluorescence. Conversely, JC-1 appeared in the mitochondrial cytoplasm and generated green fluorescence in unhealthy mitochondria. Consequently, analyzing the ratio of red/green JC-1 fluorescence provided an indication of MMP alterations. The obtained results were subsequently analyzed using Image J software (Version 1.53c, National Institutes of Health.USA).

Assessment of mitochondrial Ca^{2+} levels: Mitochondrial Ca^{2+} was detected using Rhod-2AM staining (Red, YEASEN, Shanghai, China) as previously reported [27]. HK-2 cells were incubated with Rhod-2AM (1uM) at 37 °C for 30 min. The cells were then washed with PBS for three times. In addition, MitoTracker-Green (100 nM, Green, YEASEN, Shanghai, China) was used to mark the mitochondria. The Rhod-2 AM fluorescence degree was evaluated under the laser scanning confocal microscope (Zeiss).

Detection of the mitochondrial respiratory chain enzymes complex V (ATPase) activity and mitochondria ATP levels: The ATPase activity was assessed using a mitochondrial complex V/ATP synthase activity assay kit (AC-10311, ACMEC Biochemical, Shanghai, China) in accordance with the manufacturer's instructions and previous studies [28]. In summary, HK-2 cells were placed in cell-culture dishes, and the experimental groups were treated with either paricalcitol or Mfn2 siRNA. All groups were then subjected to centrifugation at 11,000g for 15 min. The ATPase activity was determined at 660 nm using a spectrophotomer. The enzyme activity was reported as U/mg protein, with the control group's average ATPase activity serving as the reference. Additionally, the levels of mitochondria ATP in the HK-2 cells was measured using an ATP activity assay kit (S0026, Beyotime Biochemical, Shanghai, China) following the manufacturer's instructions and previous reports [29]. Briefly, the harvested HK-2 cells were lysed with a lysis buffer, and then centrifuged at 12,000g for 5 min at 4 °C. The ATP level was determined by mixing 50ul of the supernatant with 50 μl of luciferase reagent using a microplate luminometer.

Mitochondrial isolation: The mitochondria isolation kit for tissue (HY–K1061) and mitochondrial isolation kit for cultured cells (HY–K1060) were obtained from MedChemExpress LLC (NJ, USA).

The mitochondria was isolated using as previously reported and manufacturer' s protocol [30]. Briefly, the fresh renal tissue or HK-2 cells were put in ice cold isolation buffer, then the sample was centrifuged twice for 5 min. Supernatant was transferred to new tubes and

centrifuged at 12 000g for 10 min, then after resuspended, pooled, and re-centrifuged, the mitochondrial precipitation was resuspended using 100ul store buffer. Isolated mitochondria were then stored on ice before the start of further research.

Statistical analysis: All data were presented as mean ± standard deviation (SD) (n), Unpaired or paired Student's t-test, one-way ANOVA and two-way ANOVA were used for statistical comparisons among different groups. A value of $P < 0.05$ was set as statistical significance. All study results were analyzed using the SPSS 22.0 and GraphPad Prism 7.0 software.

3. Results

3.1. Calcitriol alleviated general parameters and renal tubulointerstitial lesion of diabetic rats

24 weeks after induction of diabetes, none of the rats died. Some biochemical parameters were observed in this study. STZ-induced diabetic rats developed significant hyperglycemia but calcitriol treatment had no effects on blood glucose level (28.1 ± 0.9 mmol/L(6) vs. 26.3 ± 1.3 mmol/L(6) (Fig. 1A), body weight (232.5 ± 18.3g (6) vs. 220.5 ± 15.7g (6) (Fig. 1B) and the ratio of kidney weight/body weight (7.5 ± 0.5 mg/g (6) vs. 7.2 ± 0.6 mg/g (6) (Fig. 1C). We found that the levels of serum BUN (Fig. 1E) and Scr (Fig. 1F) were increased in STZ induced diabetic rats (17.5 ± 1.7 mmol/L (6) and 33.8 ± 2.1 μmol/L (6) respectively), in addition, the level of 24 h urinary protein was elevated

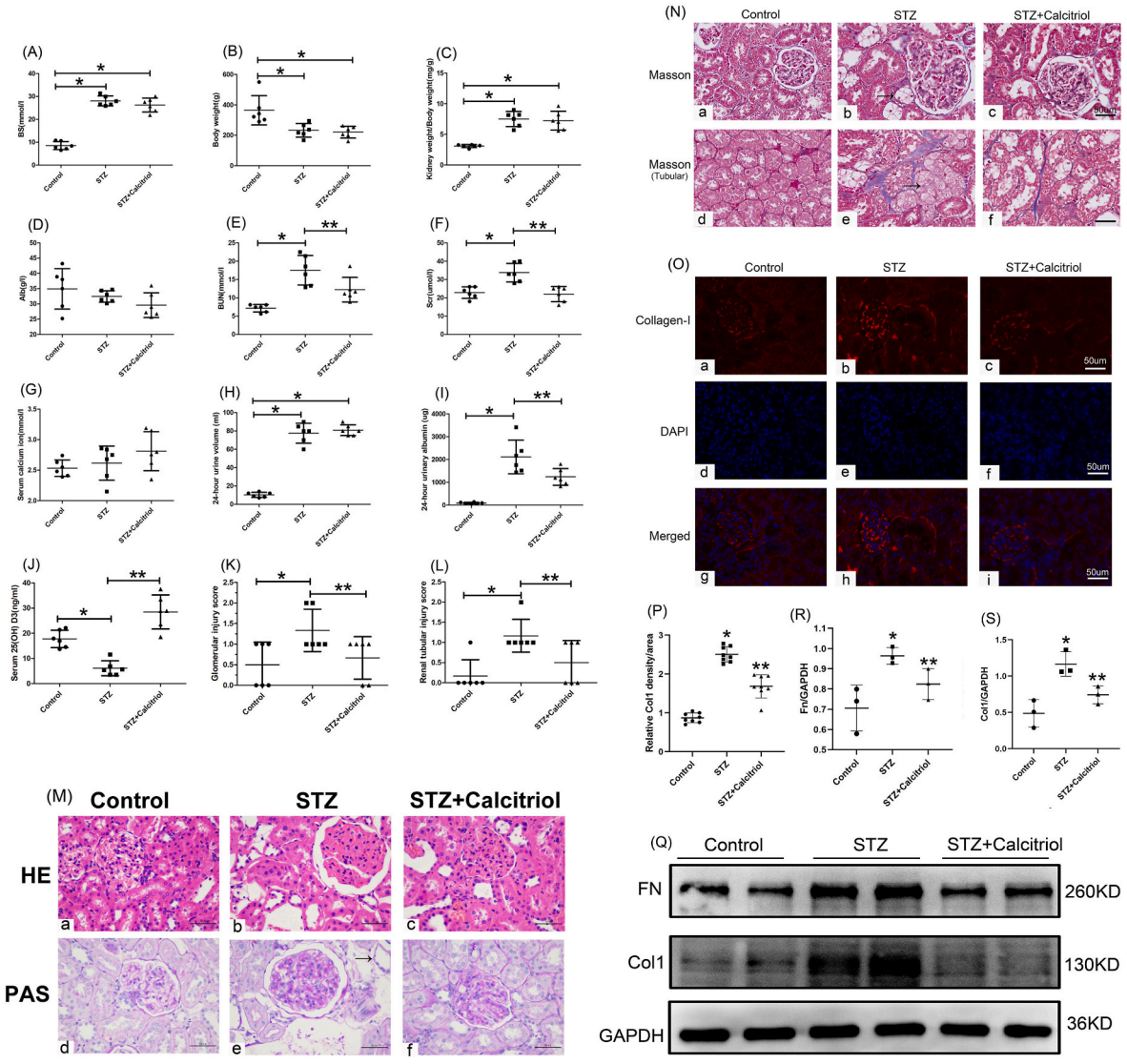

Fig. 1. Calcitriol treatment relieved biochemical parameters and renal pathological injury in diabetic rats.
A–C: Blood glucose, Body weight, Kidney weight/body weight ratio levels of different groups rats. D-G. Serum Alb, BUN, Scr and serum calcium ion levels of three groups rats. H. 24 h urine volume levels of three groups rats. I.24 h urinary albumin content of three groups rats. J.Serum levels of 25(OH)D3 in rats. K. Glomerular injury scores. L. Renal tubulo-interstitial injury scores. The values were reported as the mean ± SD (n), n = 6, *P < 0.05 vs. control group, **P < 0.05 vs. STZ group. M. HE staining (a–c) and PAS staining (d–f) of renal sections (magnification × 400, scale bar: 50um). N. Masson staining of renal tissue, the arrows indicated examples of damaged tubules (magnification × 400, scale bar: 50um). O. IF staining of Col-1 in rats renal tissue (magnification × 400, scale bar: 50um). P. Semi-quantification analysis of IF staining for Col1. Values were presented as the mean ± SD (n), n = 6, *P < 0.05 vs. control group, **P < 0.05 vs. STZ group. Q. Western blot detection of FN (upper panel) and Col1 (lower panel) expression in renal tissue. R–S. Quantitative analysis of the Western blot results, GAPDH was used as the internal control. FN to GAPDH (R), Col1 to GAPDH (S). The values were reported as the mean ± SD (n), n = 3, *P < 0.05 vs. control group, **P < 0.05 vs. STZ group.

significantly in STZ rats (2115 ± 300.7ug (6) (Fig. 1I). Conversely, the level of serum 25 (OH) Vitamin D3 decreased significantly in diabetic rats (Fig. 1J), and calcitriol treatment could effectively restore these changes ($P < 0.05$). On the other hand, there was no obvious difference of serum Alb and calcium ion levels among three different groups (Fig. 1D and G, $P > 0.05$).

In diabetic rats, HE and PAS staining showed mesangial matrix proliferation and renal glomerular basal membrane thickening (Fig.1M). Masson staining showed various degrees of partial dilatation and vacuolar degeneration of renal tubule epithelial cells (Fig.1N). While these lesions were partially relieved by calcitriol treatment ($P < 0.05$, Fig. 1K and L). In order to analysis renal interstitial fibrosis in diabetic rats, IF staining shown that the expression of Col1 was significantly increased in STZ rats ($P < 0.05$, Fig. 1 O, P), while calcitriol treatment could partially decrease these tubulointerstitial lesions ($P < 0.05$, Fig. 1 O, P). To further confirm these findings, similar result was observed regarding Col-1 and FN protein expression by Western blot analysis (Fig. 1 Q, R, S).

3.2. Calcitriol reversed mitophagy dysfunction in STZ-induced diabetic rats

In this study, we detected the expression of some vital proteins related to mitophagy by IHC staining and Western blotting. As shown in Fig. 2A, the expression of LC3II and Pink1 decreased dramatically in the renal tubular cell of diabetic rats (Fig. 2A–b, e). While calcitriol therapy effectively augmented the expression of LC3II and Pink1 in STZ-induced diabetic rats ($P < 0.05$, Fig. 2A–c, f, C,D). To further confirm the role of calcitriol in the regulation of mitophagy under diabetic conditions, we detected the expression of other mediators of mitophagy in renal tissue, similar results was found by Western blot and quantitative analysis regarding PINK1 and LC3II protein expression (Fig. 2B–E, I, $P < 0.05$). In

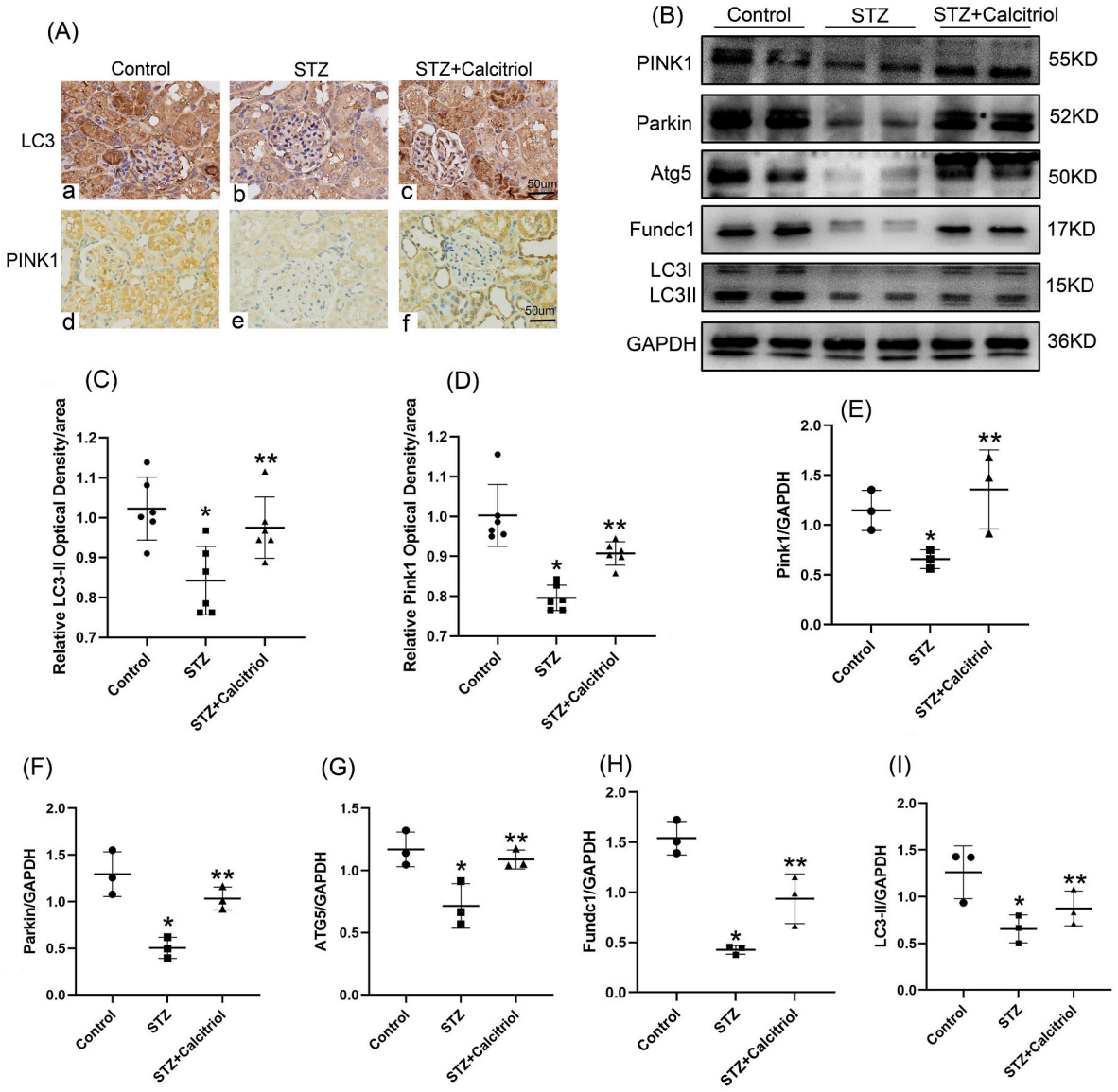

Fig. 2. Calcitriol treatment relieved mitophagy dysfunction in vivo.
A. IHC staining for LC3 (upper panel) and PINK1 (lower panel) (magnification ×400, scale bar: 50um). B.Western blot analysis of PINK1 (upper panel), Parkin, Atg5, Fundc1 (middle panels) and LC3II (bottom panel) expression in various groups of renal tissue. C-D. Quantitative analysis for the IHC staining for LC3II (C) and PINK1 (D). Values were presented as the mean ± SD (n), n = 6, *$P < 0.05$ vs. control group, **$P < 0.05$ vs. STZ group. E-I. Quantitative analysis of the Western blot results, PINK1 to GAPDH (E), Parkin to GAPDH (F), Atg5 to GAPDH (G), Fundc1 to GAPDH (H), LC3II to GAPDH (I). *$P < 0.05$ vs. control group, **$P < 0.05$ vs. STZ group. The values were reported as the mean ± SD (n), n = 3. (For interpretation of the references to color in this figure legend, the reader is referred to the Web version of this article.)

addition, STZ led to obvious declines in the expression of Parkin, Atg5, and Fundc1. Further analysis confirmed the up-regulation of Parkin, Atg5, and Fundc1 by calcitriol therapy (Fig. 2B–F, G, H, $P < 0.05$). Collectively, these findings indicated that VDR agonist calcitriol could effectively ameliorate mitophagy dysfunction in renal tissue of diabetic rats.

3.3. Calcitriol activated VDR and regulated the expression of mitochondrial fission or fusion factors in STZ-induced diabetic rats

IHC staining was performed for VDR and Mfn2 in Fig. 3A, Mfn2 was a vital regulatory factor for mitochondrial fusion and MAMs integrity. The expression of renal VDR was decreased in STZ induced diabetic rats (Fig. 3A–b). Furthermore, VDR was mainly expressed in the nucleus of renal tubular cells. Similarly, the expression level of Mfn2 was also significantly decreased (Fig. 3A–e). Quantitative analysis of IHC optical density showed that calcitriol treatment effectively augmented the

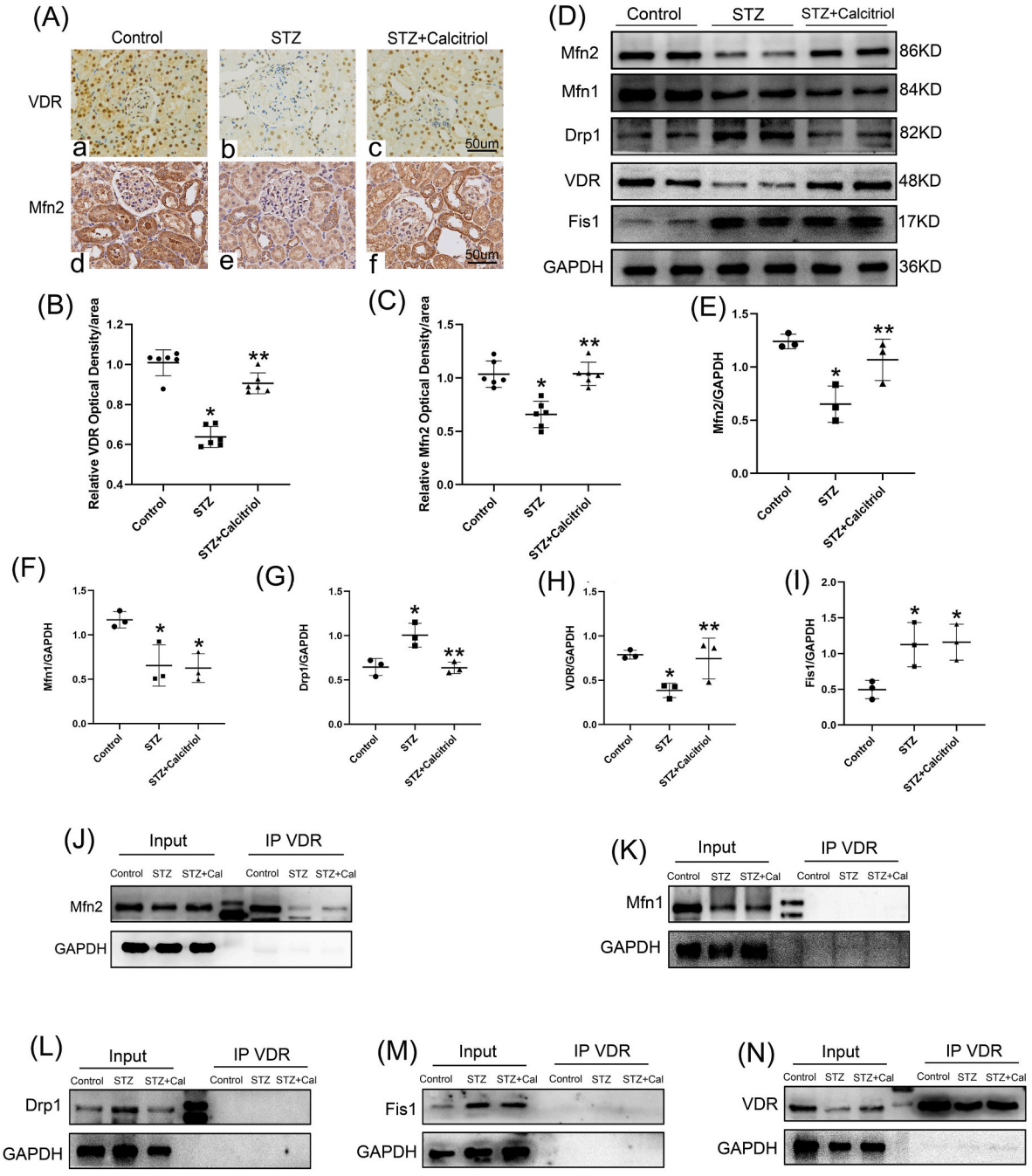

Fig. 3. Renal VDR and mitochondrial fission or fusion factors expression in diabetic rats.
A. IHC staining for VDR (upper panel) and Mfn2 (lower panel) (magnification ×400, scale bar: 50um). B–C. Quantitative analysis for the IHC staining of VDR (B) and Mfn2 (C). *$P < 0.05$ vs. control group, **$P < 0.05$ vs. STZ group. The values were reported as the mean ± SD (n), n = 6. D. Western blot analysis of Mfn2 (upper panel), Mfn1,Drp1, VDR (middle panels) and Fis1 (bottom panel) expression. E-I. Densitometric quantitative analysis of the Western blotting results, Mfn2 to GAPDH (E), Mfn1 to GAPDH (F), Drp1 to GAPDH (G), VDR to GAPDH (H), Fis1 to GAPDH (I). *$P < 0.05$ vs. control group, **$P < 0.05$ vs. STZ group, values were presented as the mean ± SD (n), n = 3. N. CO-IP analysis of VDR interacting with Mfn2 (J), Mfn1(K), Drp1(L), Fis1(M) or VDR (N) in renal tissue of various groups rat.

expression of VDR and Mfn2 in diabetic rats (Fig. 3A–c, f, B,C, $P < 0.05$). To confirm these findings, the protein expression of VDR and other mitochondrial fission regulatory factors were detected using Western blot analysis, it showed the expression of Mfn2, Mfn1 and VDR was significantly decreased in diabetic rats than that in the control group ($P < 0.05$, Fig. 3D, E, F, H), but the expression levels of Drp1 and Fis1 were significantly increased in the STZ induced diabetic group ($P < 0.05$, Fig. 3D–G, I). Further quantitative analysis of Western blot showed the up-regulation of Mfn2 and VDR while down-regulation of Drp1 by calcitriol therapy (Fig. 3D, E, H, G, $P < 0.05$). But there was no significant difference in the expression of Mfn1 and Fis1 between the calcitriol treatment group and diabetic group ($P > 0.05$, Fig. 3D–F, I). To further

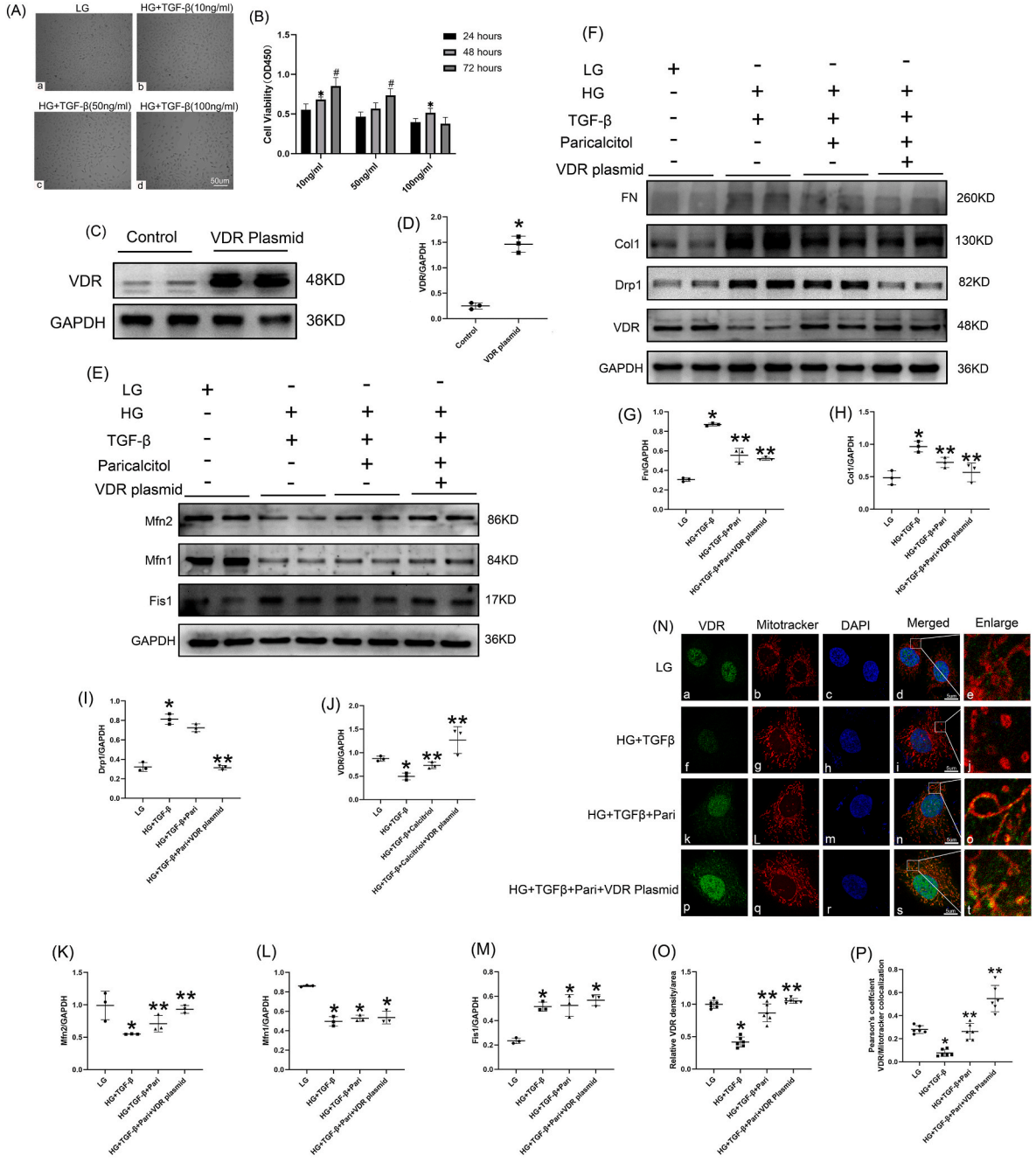

Fig. 4. Effects of VDR agonist and VDR plasmid on FN, Col1, Drp1, Mfn1, Mfn2, Fis1 protein expression in vitro.
A.HK-2 cells morphology in different concentrations of TGF-β and HG (magnification × 400). B.CCK-8 assay to detect the proliferation and viability of HK-2 cells under HG/TGF-β stimulation. C.Western blot analysis of VDR protein expression in the HK-2 cells. D. Quantitative analysis of Western blot results, *P < 0.05 vs. control groups, values were presented as the mean ± SD (n), n = 3. E. Western blot analysis of Mfn2 (upper panel), Mfn1(middle panel), and Fis1 (bottom panel) protein expression in HK-2 cells. F. Western blot analysis of FN (upper panel), Col-1, Drp1 (middle panel), and VDR (bottom panel) protein expression in HK-2 cells of various groups. G-M. Quantitative analysis of the Western blot results: FN to GAPDH (G), Col1 to GAPDH (H), Drp1 to GAPDH (I), VDR to GAPDH (J), Mfn2 to GAPDH (K), Mfn1 to GAPDH (L) and Fis1 to GAPDH (M). *P < 0.05 vs. LG group, **P < 0.05 vs. HG + TGF-β group, values were presented as the mean ± SD (n), n = 3. N. Confocal microscopy detection of VDR (right panel, green), mitochondria (middle panel, red), and nucleus (DAPI, blue) in HK-2 cells (magnification × 630, scale bar: 5 μm). O. Quantitative analysis of VDR fluorescence density. *P < 0.05 vs. LG group, **P < 0.05 vs. HG + TGF-β group. P. Pearson's co-localization analysis between VDR and Mitotracker, *P < 0.05 vs. LG group, **P < 0.05 vs. HG + TGF-β group, the values were reported as the mean ± SD (n), n = 6. (For interpretation of the references to color in this figure legend, the reader is referred to the Web version of this article.)

explore the interaction between VDR and mitochondrial fission or fusion factors, we hypothesized that VDR interacted with Mfn1 or Drp1 to regulate mitochondrial fission or fusion. CO-IP analysis was performed in renal tissue of various group, CO-IP results demonstrated that the anti-VDR antibody pulled down both VDR and Mfn2 proteins (Fig. 3J–N). Conversely, Western blot analysis indicated that anti-VDR antibody could not pull down Mfn1, Drp1 and Fis1 proteins (Fig. 3K, L, M). These results showed a physical interaction between VDR and Mfn2.

3.4. VDR down-regulated fibrosis related factors and mitochondrial fission in HK-2 cells exposed to HG/TGF-β conditions

Phase-contrast light microscopy detection showed that the morphology of HK-2 cells was changed remarkably under the stimulation of HG and TGF-β(Fig. 4A a-d).

Then, we performed a CCK-8 assay to explore the impact of TGF-βon the proliferation and viability of HK-2 cells. As shown in Fig. 4B, both low concentration of TGF-β(10 ng/ml) and medium concentration of TGF-β(50 ng/ml) treatment could elevate cell proliferation and viability from 24 to 72 h. On the contrary, the most high concentration of TGF-β(100 ng/ml) treatment markedly reduced cell proliferation and viability at 72 h. Based on these results, moderate concentration of TGF-β(50 ng/ml) and high glucose (30 mM) stimulation were combined used to mimic diabetic renal tubular cell injury status in our study.

To further explore the impact of VDR on mitochondrial fission, we applied the VDR overexpression plasmid in this study. In HK-2 cells after transfection with the VDR plasmid, Western blot analysis demonstrated a obvious increase in the expression of VDR ($P < 0.05$, Fig. 4C–D). Then high concentrations of glucose (30 mM) and TGF-β (50 ng/ml) were using to stimulate HK-2 cells as a mimic way of DN condition in vitro. As expected, Western blot detection indicated that the protein levels of FN, Col-1, Drp1 and Fis1 were up-regulated significantly in HK-2 cells under HG/TGF-β condition ($P < 0.05$, Fig. 4E, F, G, H, I, M). Conversely, the expression levels of VDR, MFN2 and Mfn1 was down-regulated evidently in HK-2 cells under HG/TGF-β condition ($P < 0.05$, Fig. 4E, F, J, K, L). Further quantitative analysis of Western blot showed the up-regulation of VDR and Mfn2 while down-regulation of FN, Col1, and Drp1 by VDR overexpression plasmid and paricalcitol therapy (Fig. 4E, F, G, H, I, J, K, $P < 0.05$). On the contrary, regarding the expression of Mfn1 and Fis1, there was no significant difference between VDR overexpression plasmid and paricalcitol treatment group and HG/TGF-βgroup ($P > 0.05$, Fig. 4E, L, M).

In order to further explore the regulatory effect of VDR on mitochondria function, IF co-staining of VDR and mitochondria was performed, IF staining showed that VDR was mainly expressed in the nucleus while minority expressed in the cytoplasm of HK-2 cells. After the stimulation of HG and TGF-β, the expression of VDR was significantly decreased, and along with obvious increased mitochondrial fragmentation (Fig. 4N–f, g). After VDR overexpression plasmid and

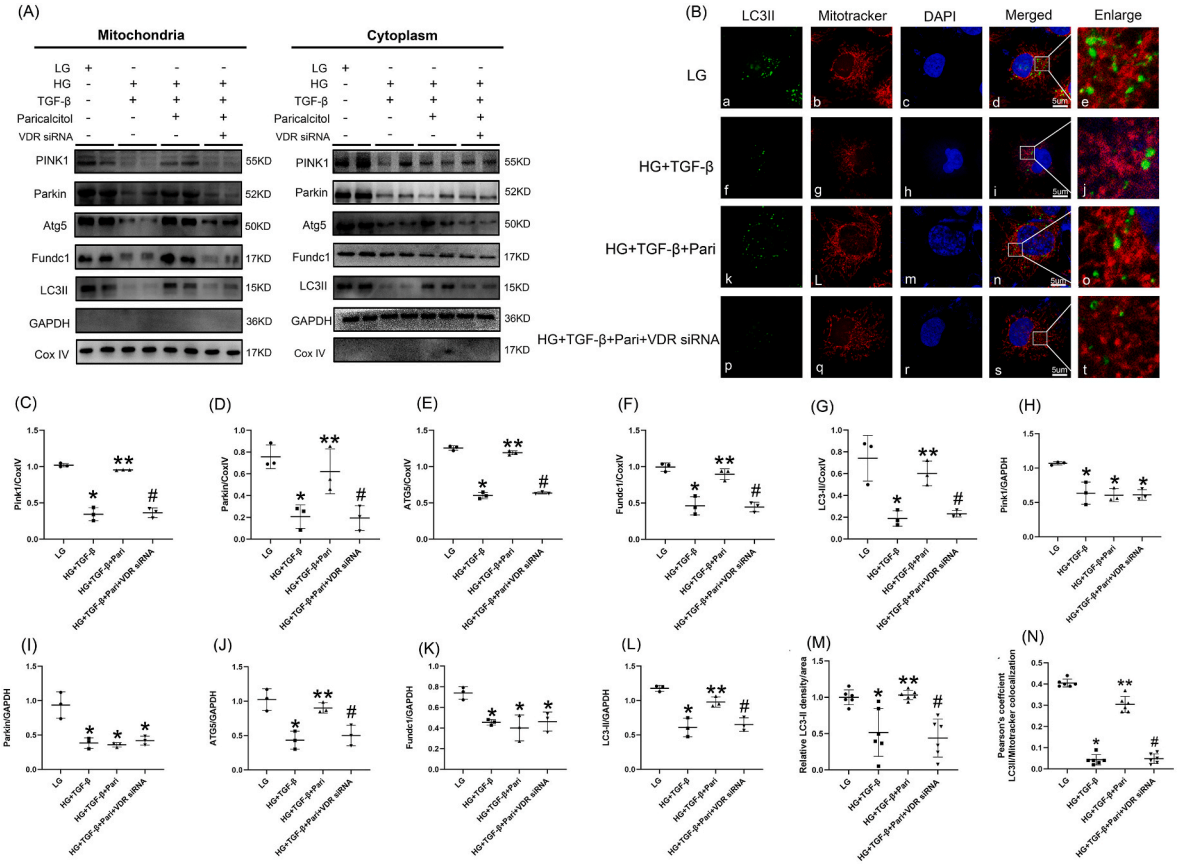

Fig. 5. VDR restored mitophagy in HK-2 cells under HG/TGF-β stimulation.
Western blot analysis of mitochondria proteins (left panels) and cytoplasm proteins (right panels) including PINK1 (upper panel), Parkin, Atg5, Fundc1 (middle panels) and LC3II (bottom panel). B. Confocal microscopy detection of LC3II expression and mitochondrial morphology in HK-2 cells. C-L. Quantitative analysis of the Western blot results, Pink1 to CoxIV (C), Parkin to CoxIV (D), Atg5 to CoxIV (E), Fundc1 to CoxIV (F), LC3II to CoxIV (G), Pink1 to GAPDH (H), Parkin to GAPDH (I), Atg5 to GAPDH (J), Fundc1 to GAPDH (K), LC3II to GAPDH (L), *$P < 0.05$ vs. LG group, **$P < 0.05$ vs. HG + TGF-β group, $^{\#}P < 0.05$ vs. HG + TGF-β+Pari group, values were presented as the mean ± SD (n), n = 3. M. Quantitative analysis of LC3II fluorescence optical density. N.Pearson's co-localization analysis between VDR and Mitotracker, *$P < 0.05$ vs. LG group, **$P < 0.05$ vs. HG + TGF-β group, $^{\#}P < 0.05$ vs. HG + TGF-β+ Pari group, values were presented as the mean ± SD (n), n = 6. (For interpretation of the references to color in this figure legend, the reader is referred to the Web version of this article.)

paricalcitol treatment, we found that the VDR expression and thread-like mitochondria was increased significantly (Fig. 4N–k, l, p, q, O). In addition, the colocalization of VDR (labeled with green) and mitochondria (labeled with red) was detected by confocal laser scanning microscopy. Treatment with VDR overexpression plasmid and paricalcitol for 72 h could promote the colocalization of VDR and mitochondria in HK-2 cells ($P < 0.05$, Fig. 4N–P).

3.5. VDR restored mitophagy in HK-2 cells exposed to HG/TGF-β conditions

Mitochondria and cytoplasm protein of HK-2 cells were extracted to perform Western blot analysis. In the group of HK-2 cells exposed to HG/TGF-βstimulation, the mitochondria and cytoplasm protein expression of Pink1, Parkin, Atg5, Fundc1 and LC3II were all decreased significantly ($P < 0.05$, Fig. 5 A, C-L), and VDR agonist paricalcitol treatment promoted an observably increase in the mitochondrial protein levels of Pink1, Parkin, Atg5, Fundc1 and LC3II ($P < 0.05$, Fig. 5A–C-G). Additionally, the paricalcitol induced the upregulation mitochondrial protein of Pink1, Parkin, Atg5, Fundc1 and LC3II was partially abrogated by VDR siRNA treatment ($P < 0.05$, Fig. 5A–C-G). On the other side, paricalcitol treatment promoted an obviously increase in cytoplasmic protein levels of Atg5 and LC3II, but had no significant effect on cytoplasmic protein levels of Pink1, Parkin and Fundc1($P > 0.05$, Fig. 5A–J, L, H, I, K). As LC3II was a vital marker of autophagy, IF staining of LC3II and mitochondria was performed, as exhibited in

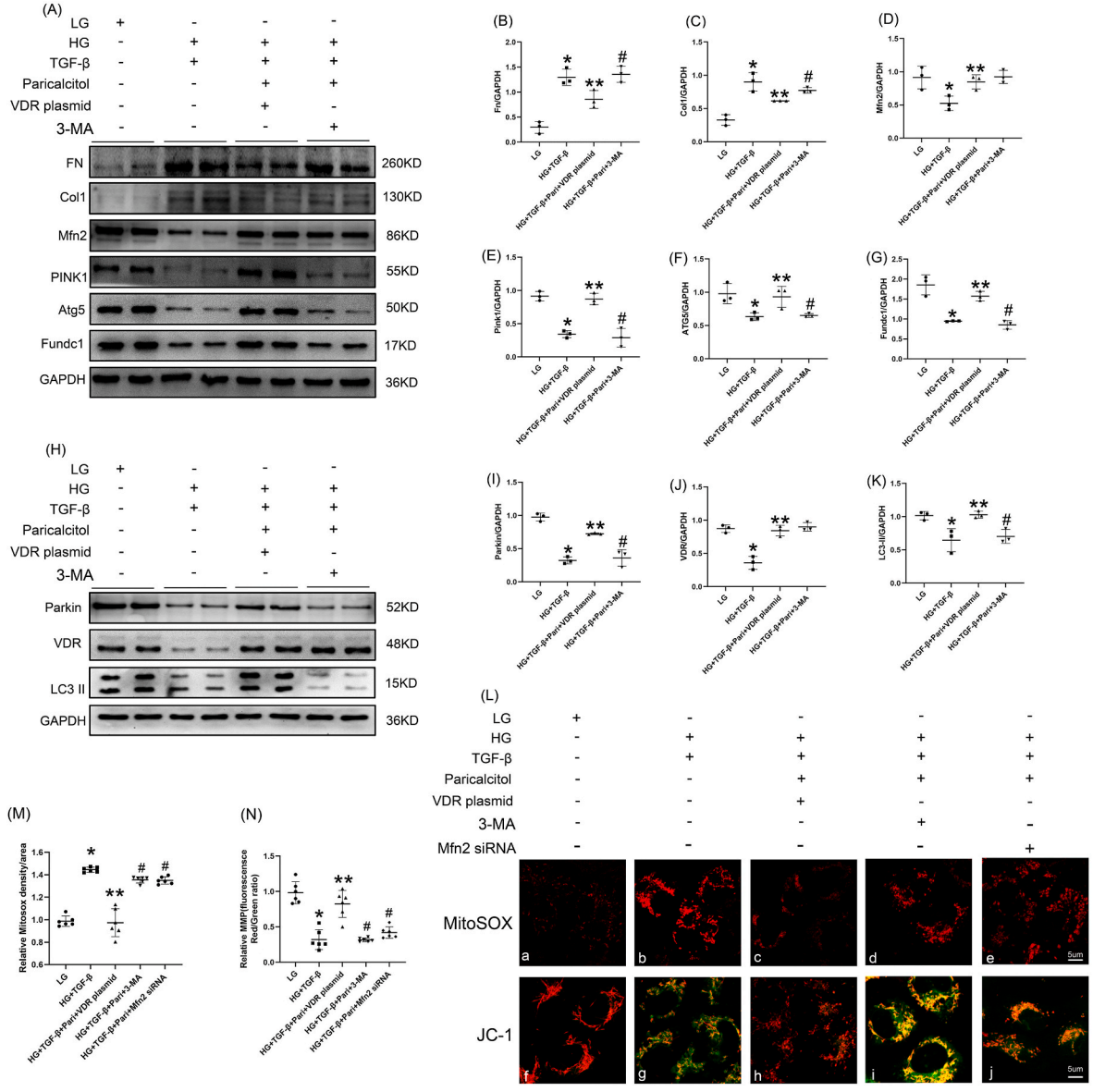

Fig. 6. VDR activated mitophagy was beneficial for ameliorating fibrosis and mitochondrial function.
A.Western blot analysis of FN, Col1, Mfn2, Pink1, Atg5 and Fundc1protein expression in the HK-2 cells. B-G. Quantitative analysis of Western blot results, FN to GAPDH (B), Col1 to GAPDH (C), Mfn2 to GAPDH (D), Pink1 to GAPDH (E), Atg5 to GAPDH (F) and Fundc1 to GAPDH (G), *P < 0.05 vs. LG group, **P < 0.05 vs. HG + TGF-β group, #P < 0.05 vs. HG + TGF-β+Pari + VDR plasmid group, values were presented as the mean ± SD (n), n = 3. H. Western blot analysis of Parkin, VDR, and LC3 II expression. I–K. Quantitative analysis of Western blot results: Parkin to GAPDH (I), VDR to GAPDH (J), LC3II to GAPDH (K), *P < 0.05 vs. LG group, **P < 0.05 vs. HG + TGF-β group, #P < 0.05 vs. HG + TGF-β+Pari + VDR plasmid group, values were presented as the mean ± SD (n), n = 3. L. MitoSOX Red and JC-1 staining (magnification × 630, scale bar: 5 μm). M. Semi-quantitative analysis of MitoSox Red fluorescence optical density. N. Semi-quantitative analysis of MMP. *P < 0.05 vs. LG group, **P < 0.05 vs. HG + TGF-β group, #P < 0.05 vs. HG + TGF-β+Pari + VDR plasmid group, values were presented as the mean ± SD (n), n = 6. (For interpretation of the references to color in this figure legend, the reader is referred to the Web version of this article.)

Fig. 5B, HG/TGF-βstimulation significantly decreased the expression of LC3II, and accompanied by obviously increased mitochondrial fragmentation in HK-2 cells (Fig. 5B–M). Furthermore, the colocalization of LC3II and mitochondria was detected by confocal laser scanning microscopy. Treatment of HK-2 cells with paricalcitol for 72 h could effectively promote the colocalization of mitochondria and LC3II and partially reverse mitochondrial fragmentation ($P < 0.05$, Fig. 5B–N). While pretreatment with VDR siRNA could partially abolish the up-regulated expression of LC3II in mitochondrial induced by paricalcitol ($P < 0.05$, Fig. 5B, M, N). These results indicated that activation of VDR could up-regulate mitophagy in HK-2 cells under HG/TGF-βstimulation.

3.6. VDR ameliorated fibrosis and mitochondrial dysfunction partially through regulation of mitophagy

In this section, we sought to determine whether VDR agonist treatment could effectively alleviate fibrosis and mitochondrial function through activating mitophagy. As shown in Fig. 6, Western blot analysis demonstrated that the protein expression of FN and Col-1 were up-regulated significantly in HK-2 cells after the stimulation with HG/TGF-β($P < 0.05$, Fig. 6A, B, C). On the contrary, the expression levels of VDR, MFN2, PINK1, Parkin, Atg5, Fundc1 and LC3II were down-regulated evidently in HK-2 cells under HG/TGF-β condition ($P < 0.05$, Fig. 6A–D, E, F, G, H, I, J, K). Further quantitative analysis of Western blot showed the down-regulation of FN and Col1 while up-regulation of PINK1, Parkin, Atg5, Fundc1 and LC3II by VDR overexpression plasmid and paricalcitol therapy was abolished by pretreatment with autophagy inhibitor 3-MA ($P < 0.05$, Fig. 6A, B, C, E, F, G, H, I, K). However, 3-MA had no significant impact on the expression of Mfn2 and VDR ($P > 0.05$, Fig. 6A–D,H,J), it indicated that VDR and Mfn2 were upstream regulatory factors of autophagy.

We used MitoSOX red and JC-1 staining to explore the changes of mitochondrial function in vitro. MitoSOX red staining revealed a significant increase of mitochondrial ROS level in HK-2 cells under HG/TGF-β condition ($P < 0.05$, Fig. 6L and M). Besides, JC-1 staining showed that HG/TGF-βstimulation could significantly down-regulate the level of MMP in HK-2 cells. Moreover, These changes were effectively reversed after pretreatment with paricalcitol and VDR overexpression plasmid ($P < 0.05$, Fig. 6L, M, N). Further analysis showed that the down-regulation of mitochondrial ROS while up-regulation of MMP by VDR overexpression plasmid and paricalcitol therapy was abolished by the pretreatment with 3-MA or Mfn2 siRNA ($P < 0.05$, Fig. 6L, M, N).

3.7. VDR restored mitophagy partially through Mfn2-MAMs-Fundc1 pathway

Mfn2 siRNA were used to further explore whether Mfn2 was associated with VDR agonist induced up-regulation of mitophagy. First, similar to the previous result, We found that the protein expression of Mfn2 and VDR were decreased significantly in HK-2 cells under HG/TGF-βstimulation, while pretreatment with paricalcitol could increase the protein levels of Mfn2 and VDR ($P < 0.05$, Fig. 7A, B, C). Further quantitative analysis showed the up-regulation of Mfn2 by paricalcitol therapy was abrogated by Mfn2 siRNA ($P < 0.05$, Fig. 7A and B). However, Mfn2 siRNA had no remarkable impact on the upregulatd expression of VDR ($P > 0.05$, Fig. 7A–C), it indicated that VDR was an upstream regulatory factor of Mfn2. To confirm the regulative role of VDR-Mfn2 pathway on mitophagy, mitochondria and cytoplasm protein of HK-2 cells were extracted to perform Western blot analysis respectively. It showed that the expression levels of Pink1, Parkin, Fundc1 and LC3II were significantly down-regulated both in the cytoplasm and mitochondria under HG/TGF-βstimulation ($P < 0.05$, Fig. 7D-M), and paricalcitol treatment promoted an obvious increase in the mitochondrial protein levels of Pink1, Parkin, Fundc1 and LC3II ($P < 0.05$, Fig. 7 D, F, G, H, I). Conversely, paricalcitol therapy had no significant impact on the cytoplasmic protein levels of Pink1, Parkin and Fundc1 ($P > 0.05$, Fig. 7 E, J, K, L). In further study we also found that the up-regulated mitochondrial expression of Pink1, Parkin, Fundc1 and LC3II induced by paricalcitol were significantly abolished by Mfn2 siRNA transfection ($P < 0.05$, Fig. 7 D, F, G, H, I).

Double IF staining showed that the co-localization of Mfn2 and Fundc1 in HK-2 cells (Fig. 7N). The expression levels of Fundc1 and Mfn2 were both significantly reduced under HG/TGF-βstimulation, while pretreatment with paricalcitol could increase Fundc1 and Mfn2 expression. These changes and the colocalization of Fundc1 and Mfn2 were partially abolished after Mfn2 siRNA transfection ($P < 0.05$, Fig. 7 N, O, P, Q). As Mfn2 was a vital regulator of MAMs, in this study, we observed the changes of mitophagy and MAMs integrity both in vivo and in vitro. As exhibited in Fig. 7R, under the detection of TEM, the morphology of mitochondria in tubular cell of diabetic rat changed obviously, mitochondria swelling and fission was found (Fig. 7R–e,f,g). For another, conspicuous mitochondrial autophagosome was found in the renal tubular cell of diabetic rat treated with calcitriol (Fig. 7R–i, j, k). Furthmore, we found that MAMs was decreased in diabetic rats shown as red dots, while calcitriol therapy could increase MAMs integrity ($P < 0.05$, Fig. 7R–c, g, k, U). In vitro studies, TEM analysis was performed. In the HK-2 cells after HG/TGF-β intervention, vacuolated and swollen mitochondria, as well as MAMs integrity destroy were found. After treatment with the paricalcitol, the MAMs contact and mitochondrial autophagosome were partially increased, but these beneficial changes were abolished by Mfn2 siRNA transfection ($P < 0.05$, Fig. 7S and V). Besides, MitoTracker and ER-blue IF double staining was used to detect MAMs integrity, it showed that the colocalization between ER and mitochondria was decreased after HG/TGF-β stimulation in HK-2 cells ($P < 0.05$, Fig. 7Te-h, W), while paricalcitol therapy could partially increase MAMs integrity ($P < 0.05$, Figs.7Ti-l, W), but these effects were abolished after Mfn2 siRNA transfection ($P < 0.05$, Figs.7Tm-p, W). Conversely, autophagy inhibitor 3-MA had no significant effect on MAMs integrity ($P > 0.05$, Figs.7Tq-t, W). On the basis of these results, we hold the opinion that the VDR-Mfn2 could partially regulate mitophagy through the MAMs and Fundc1 pathways.

3.8. VDR restored MAMs integrity partially through Mfn2-SRECA2 coupling

In this study, Mitotracker Green and Rhod-2 AM were used to detect mitochondrial Ca^{2+} levels. As shown in Fig. 8, the fluorescence intensity level of Rhod-2 AM, the colocalization of Mitotracker Green and Rhod-2 AM were both significantly reduced under HG/TGF-βintervention, whereas IF staining showed that pretreatment with paricalcitol increased Rhod-2 AM fluorescence intensity. These changes and the fluorescence colocalization of Mitotracker Green and Rhod-2 AM were partially abolished after Mfn2 siRNA transfection ($P < 0.05$, Fig. 8A, B, C). It indicated that paricalcitol treatment significantly increased mitochondrial Ca^{2+} levels, a phenomenon that was accompanied by elevated MAMs integrity. Then mitochondria ATP and Complex V activity were detected to further explore intracellular mitochondrial function. HG/TGF-β intervention significantly reduced the levels of mitochondria ATP and Complex V activity. Moreover, These changes were obviously reversed after paricalcitol treatment ($P < 0.05$, Fig. 8D and E). Further analysis showed that the up-regulation of mitochondria ATP and Complex V activity by paricalcitol therapy was partially abolished by Mfn2 siRNA transfection ($P < 0.05$, Fig. 8 D, E).

Our study have shown that MAMs integrity was involved in the development of DN. Based on the latest research, ER localization of SERCA2 was a vital regulatory factor of MAMs integrity in T leukomonocyte [31]. In this study, we sought to determine whether SERCA2 from ER were involved or acted as modulators of MAMs integrity in renal tubular cell. As exhibited in Fig. 8, Western blot analysis indicated that the protein level of SERCA2 was decreased significantly both in HK-2 cells under HG/TGF-βcondition and renal tissue of STZ rats ($P <$

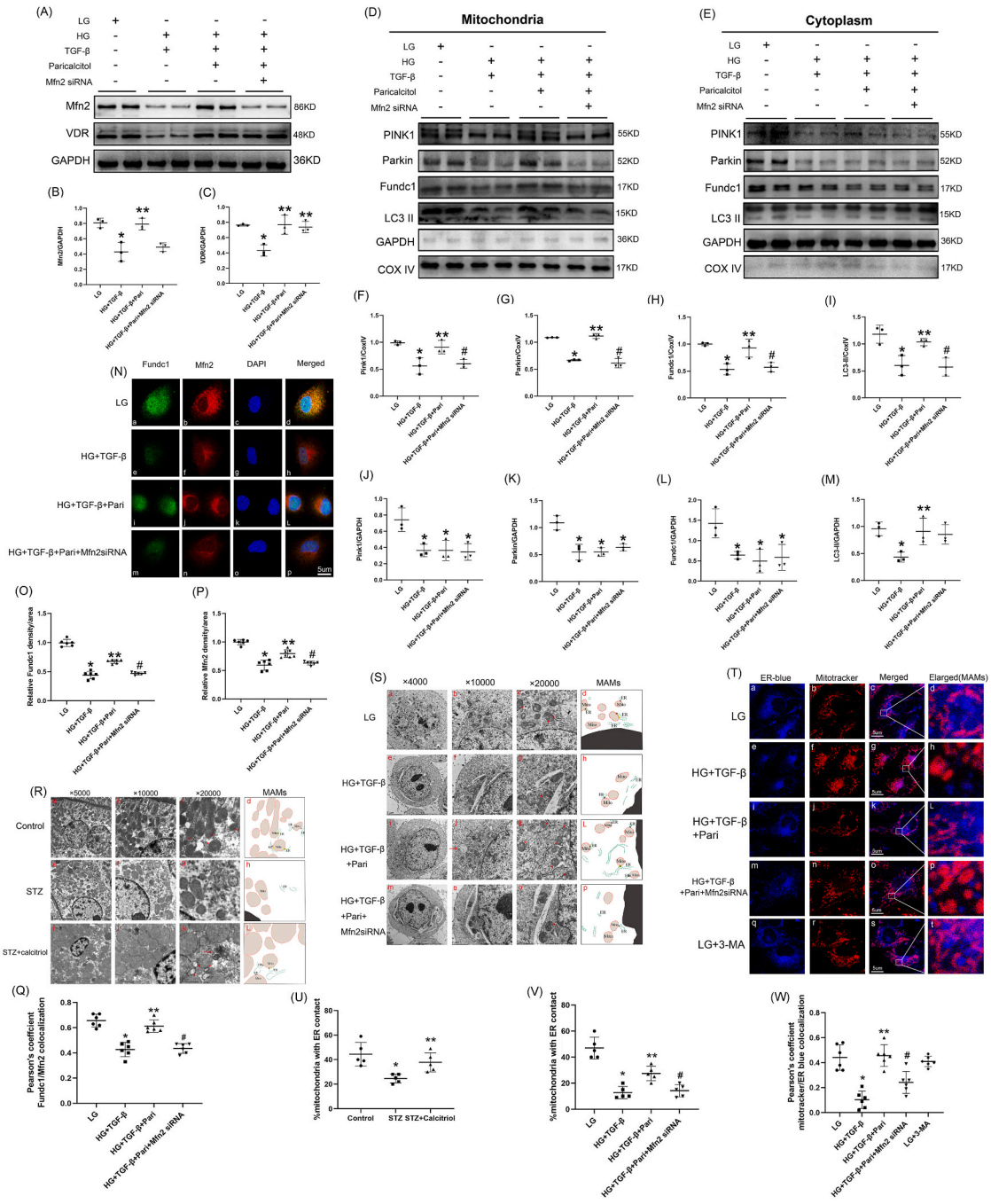

Fig. 7. VDR restored mitophagy was partially associated with MAMs integrity.
A.Western blot analysis of Mfn2 and VDR expression in HK-2 cells. B–C. Quantitative analysis of Western blot results, Mfn2 to GAPDH (B), VDR to GAPDH (C). D-E. Western blot analysis of mitochondria protein (left panels) and cytoplasm protein (right panels) including PINK1, Parkin, Fundc1 and LC3II in HK-2 cells. F-M. Quantitative analysis of the Western blot results, Pink1 to CoxIV (F), Parkin to CoxIV (G), Fundc1 to CoxIV (H), LC3II to CoxIV (I), Pink1 to GAPDH (J), Parkin to GAPDH (K), Fundc1 to GAPDH (L), LC3II to GAPDH (M). *P < 0.05 vs. LG group, **P < 0.05 vs. HG + TGF-β group, #P < 0.05 vs. HG + TGF-β+Pari group, values were presented as the mean ± SD (n), n = 3. N. Confocal microscopy analysis of Fundc1 and Mfn2 expression in HK-2 cells. O–P. Quantitative analysis of Fundc1 and Mfn2 fluorescence optical density. Q. Pearson' s co-localization analysis for Fundc1 and Mfn2. *P < 0.05 vs. LG group, **P < 0.05 vs. HG + TGF-β group, #P < 0.05 vs. HG + TGF-β+Pari group, values were presented as the mean ± SD (n), n = 6. R. TEM analysis of mitochondrial morphological changes in renal tubular cells of STZ rats. The red dots and black dots represented MAMs structure. Calcitriol treatment group exhibited conspicuous mitochondrial autophagosome (k, marked with red arrow, d, h, L. diagrammatic figures based on parallel TEM figures). S. TEM analysis for HK-2 cells of various group. The red dots and black dots represented MAMs structure (c, g, k, o, d, h, L, p), mitochondrial autophagosome was marked with red arrow (j) (d, h, L, p. diagrammatic figures based on parallel TEM figures. T. IF double staining using ER Blue (blue) and MitoTracker (red) in HK-2 cells. U.Bar graphs represented ER-mitochondrial contact sites in renal tissue, *P < 0.05 vs. control group, **P < 0.05 vs. STZ group, values were presented as the mean ± SD (n), n = 6. V.Bar graphs represented ER-mitochondrial contact sites in HK-2 cells. W. Pearson' s co-localization analysis between mitochondria and ER,*P < 0.05 vs. LG group, **P < 0.05 vs. HG + TGF-β group, #P < 0.05 vs. HG + TGF-β+Pari group, values were presented as the mean ± SD (n), n = 6. (For interpretation of the references to color in this figure legend, the reader is referred to the Web version of this article.)

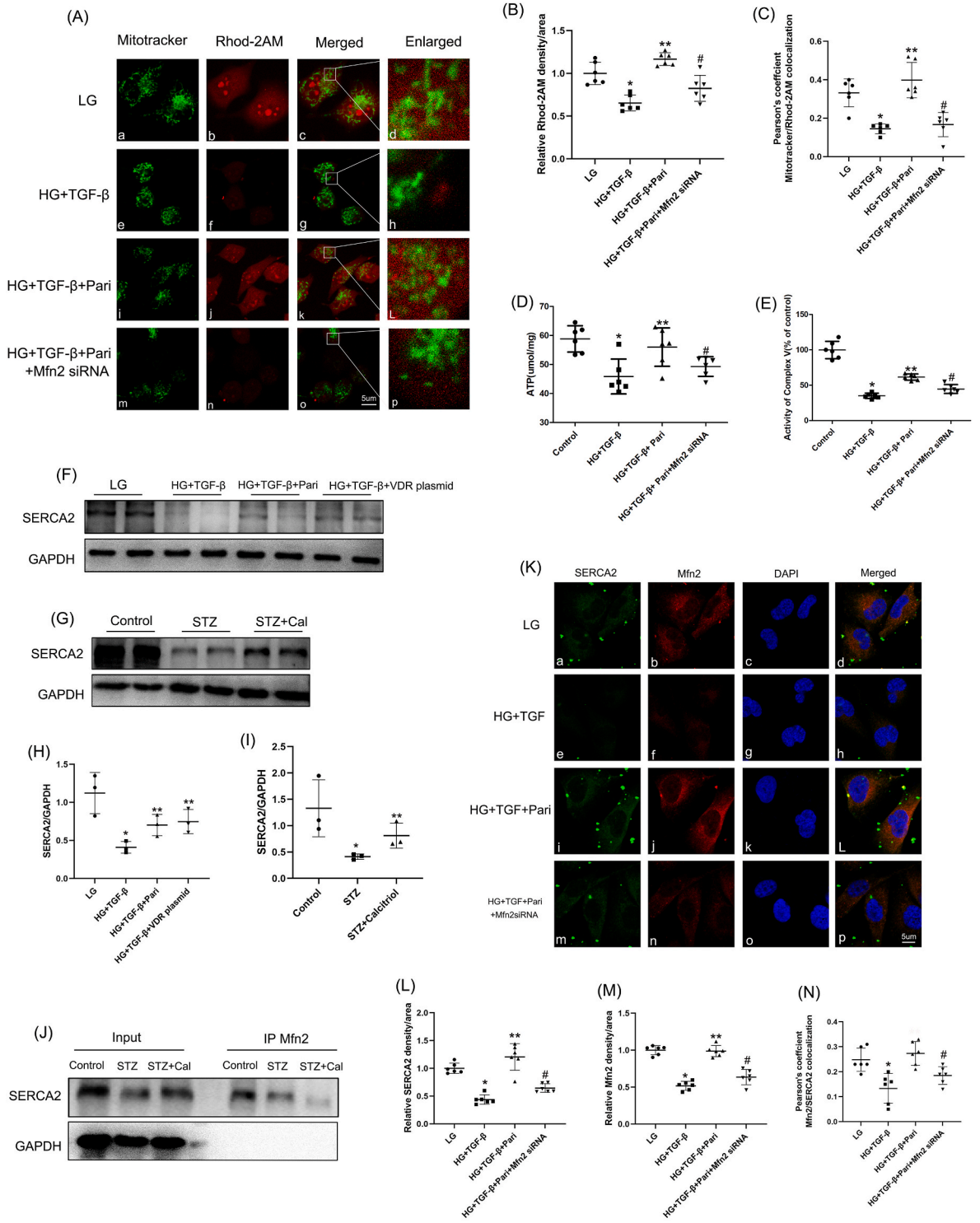

Fig. 8. Effects of VDR agonist on the levels of mitochondrial Ca^{2+}, mitochondria ATP, Complex V activity and SERCA protein expression.
A. Confocal microscopy detection of mitochondrial Ca^{2+} levels in HK-2 cells (magnification × 630, scale bar: 5 μm). B. Quantifiaction analysis of Rhod-2AM fluorescence optical density. C. Pearson's co-localization analysis between Mitotracker Green and Rhod-2 AM. D.Quantitative analysis of mitochondria ATP levels in various groups. E.Quantitative analysis of mitochondria Complex V activity levels in HK-2 cells. *P < 0.05 vs. LG group, **P < 0.05 vs. HG + TGF-β group, #P < 0.05 vs. HG + TGF-β+ Pari group, the values were reported as the mean ± SD (n), n = 6. F. Western blot analysis of SERCA2 protein expression in HK-2 cells. G. Western blot analysis of SERCA2 protein expression in renal tissue. H. Quantitative analysis of Western blot results in vitro. *P < 0.05 vs. LG group, **P < 0.05 vs. HG + TGF-β group, n = 3. I. Quantitative analysis of Western blot results in vivo, *P < 0.05 vs. control group, **P < 0.05 vs. STZ group, the values were reported as the mean ± SD (n), n = 3. J. CO-IP analysis of Mfn2 interacting with SERCA2. K. Confocal microscopy analysis of SERCA2 and Mfn2 expression in HK-2 cells (magnification × 630, scale bar: 5 μm). L-M. Quantifiaction analysis of SERCA2 and Mfn2 fluorescence optical density. N. Pearson' s co-localization analysis between SERCA2 and Mfn2, *P < 0.05 vs. LG group, **P < 0.05 vs. HG + TGF-β group, #P < 0.05 vs. HG + TGF-β+Pari group, the values were reported as the mean ± SD (n), n = 6. (For interpretation of the references to color in this figure legend, the reader is referred to the Web version of this article.)

0.05, Fig. 8 F, G, H, I). Further analysis showed the down-regulation of SERCA2 both in vivo and in vitro were effectively reversed by the pre-treatment with paricalcitol or VDR plasmid ($P < 0.05$, Fig. 8 F, G, H, I). We hypothesized that Mfn2 interacted with SERCA2 to regulate MAMs integrity, to confirm the interaction between Mfn2 and SERCA2. We then performed CO-IP analysis in renal tissue of various group. CO-IP results demonstrated that the anti-Mfn2 antibody could pull down SERCA2 proteins (Fig. 8J). Furthermore, the co-localization of Mfn2 and SERCA2 was shown in double IF staining analysis (Fig. 8K). The expression levels of SERCA2 and Mfn2 were both significantly reduced under HG/TGF-β stimulation, while pretreatment with paricalcitol could effectively increase the expression of SERCA2 and Mfn2. These changes and the fluorescence colocalization of SERCA2 and Mfn2 were partially abolished after Mfn2 siRNA transfection ($P < 0.05$, Fig. 8 K, L, M, N).

4. Discussion

The role of renal tubular epithelial cell injury and mitochondria dysfunctional has been primarily explored in our previous studies [13,32]. It has been found that abnormal mitochondrial function play a vital role in the progress of diabetic nephropathy (DN). However, the mechanism of mitochondrial function regulation in renal tubular epithelial cell under DN condition is extremely complicated and poorly understood. This study demonstrated that activation of VDR could contribute to restore MAMs integrity in renal tubular cell via modulation of the expression of Mfn2-SERCA2. In addition, VDR activation could restore mitophagy, increase the levels of MMP and mitochondrial ATP production, and restrain mitochondrial ROS in renal tubular cell of diabetic rats.

In both Western countries and our own country, DN is a significant contributor to the development of end stage renal disease (ESRD). Although traditional view indicated that glomerulosclerosis was a major feature of DN, however, recent studies suggested tubulointerstitial injury appeared early in DN, and closely correlated with renal function decline [33]. Given the importance of renal tubular cell injury in the development of renal interstitial fibrosis. Diabetic tubulopathy has become a research hotspot in recent years. In our study, obvious changes including swollen and vacuolated of renal tubular epithelial cell and mild renal tubulointerstitial fibrosis was observed in the 24-weeks diabetic rat. Previous studies indicated that the pathogenesis of diabetic tubulopathy included oxidative stress, hypoxia, inflammation, activation of profibrotic factors (e.g. TGF-β) and renin-angiotensin-aldosterone system [33]. Recent research has indicated that mitochondrial dysfunction in proximal renal tubular cells played a vital role in this process. Thus it can be seen that the in-depth study of mitochondrial quality control might promote a novel therapeutic strategy for DN.

Mitochondria was highly vulnerable to damage in stressful condition such as hyperglycemia. It was a class of highly shape-changed organelle which frequently underwent fission and fusion. In this study, we found that mitochondria was changed from a long network into small rod-like structures due to high glucose. Mitophagy, an important cellular process, targeted and removed damaged mitochondria. This was crucial because damaged mitochondria released harmful proapoptotic factors and promoted the production of ROS. Therefore, we hypothesized that mitophagy played a protective role in DN. However, excessive mitochondrial fission was associated with an increase in the production of mitochondrial ROS [13,34]. It has been demonstrated that approximately 80 % of intracellular ROS was generated in the mitochondria with the respiratory complexes [35]. Mitochondria ROS and mitophagy was constantly affecting each other. Our previous study has found that mitophagy could decrease mitochondrial ROS in STZ-induced diabetic mice [13]. Conversely, up-regulating level of ROS could promote the formation of mitophagy in colon cancer cell [36]. In this study, we further confirmed that mitophagy and mitochondrial fission disorders were associated with mitochondrial ROS overproduction, MMP reduction and renal interstitial fibrosis in diabetic rats. In addition, we found that MAMs integrity affected mitophagy, and VDR agonist could recover mitophagy partially through Mfn2-MAMs pathway.

Mitochondria-associated ER membranes (MAMs) was an unique membrane fraction between ER and mitochondria. It was involved in various metabolic disorders and neurodegenerative diseases [37]. A growing number of scholars have realized the relationship between MAMs and renal disorders (especially DN). Xue et al. found that phosphofurin acidic cluster sorting protein 2 (PACS-2) attenuated diabetic renal tubular injury via the enhancement of MAMs formation in HG-induced HK-2 cells [38]. In line with this, another study demostrated that disulfide-bond A oxidoreductase-like protein (DsbA-L) could alleviate diabetic tubular damage through maintenance of MAMs integrity [39]. Conversely, in diabetic podocytes, reduction of MAMs formation alleviated hyperglycemia-induced mitochondrial dysfunction and podocytes injury [40]. These inconsistent findings suggested that the specific pathologic effects of MAMs on DN was still needed further research. Therefore, the aim of our study was to investigate the role of VDR in MAMs integrity and whether VDR-MAMs alterations could contribute to diabetes-induced tubular cell injury. Here, we reported that activation of VDR alleviated hyperglycemia-induced mitochondrial dysfunction in renal tubular epithelial cell, accompanied by increased MAMs formation and activation of mitophagy.

The association between autophagy and MAMs was a new research hotspot. According to some recent studies, autophagy began at the ER-mitochondria coupling site [41]. In our study, we detected some key indicators of mitophagy. We found that the expression levels of Fundc1, PINK1, Parkin and LC3II in mitochondria were increased after the treatment of VDR plasmid and VDR agonist, accompanied by increased MAMs formation and Mfn2, FUNDC1 expression. FUNDC1 was a autophagy regulatory factor located in the mitochondrial outer membrane, previous study indicated that it could recruit LC3 through LC3-binding regions (LIR) to initiate mitophagy [42]. Based on recent available evidence [43,44], it was plausible that MAMs provided a platform for FUNDC1 to perform its regulatory effects on autophagy.

In addition, VDR agonist could recover mitophagy partially through Mfn2-MAMs- FUNDC1 pathway. However, future in-depth studies are needed to explore the role of MAMs on FUNDC1-mediated mitophagy.

VDR was a ligand-activated transcription factor that belonged to the nuclear receptor superfamily. The beneficial effects of vitamin D/VDR on various pathological processes have been reported [45]. Traditional research has confirmed that nuclear activated VDR could regulate various gene transcription through interacting various target gene promoters. Our team's previous research indicated that VDR activation could protect against acute kidney injury via transcriptional regulation of GPX4 [46], NF-kB p65 [47] and ATF4 [15]. In addition, it has been described the extra-nuclear distribution of VDR and in particular the recently mitochondrial localization of VDR has been reported [7]. VDR could import into mitochondria through the permeability transition pore [48]. These finding indicated that cell function might be regulated by a mitochondrial activity of VDR. In order to investigate the protective effects of VDR on mitochondria dysfunction, cultured HK-2 cells was used in vitro studies.

Previous study has confirmed that combination using TGF-β (10 ng/ml) and high glucose (30 mM) could effectively promote the production of extracellular matrix protein in HK-2 cells [14]. In order to induce a more significant profibrotic effect, high concentration of TGF-β(50 ng/ml) and high glucose (30 mM) stimulation were used to mimic diabetic renal tubular cell injury status in our study. Both VDR plasmid and VDR agonist could relieve mitochondrial swelling and reduce mitochondrial ROS. In addition, we found that VDR plasmid and paricalcitol could activate mitophagy and increase MAMs integrity. These findings suggested that VDR exerted beneficial effects on renal tubular injury in part by protective actions on the mitochondria. On the other side, the beneficial effects of VDR on ER-stress has been reported in recent years [49]. It indicated that alleviation of ER-stress by VDR might be another event needed for tubular injury protection in DN.

It has been demonstrated that the shape of mitochondria was constantly underwent fission and fusion [50]. In line with our previous studies, we found that the shape of mitochondria in HK-2 cells changed to fragment under HG stress state [51]. To maintain mitochondrial homeostasis, some key factors including fusion proteins (Mfn1, Mfn2) and fission mediators (Fis1, Drp1) controlled the balance of mitochondrial fusion and fission. It has been found that Drp1 was a vital regulator of mitochondrial fission in diabetic state, and suppressing the expression of Drp1 could be an effective therapeutic method for tubulointerstitial injury [34]. In this study, we found the expression of Mfn2 and Mfn1 were significantly decreased, while the expression of Fis1 and Drp1 were increased in renal tissue of diabetic rats. In addition, treatment with VDR agonist calcitriol could regulate the expression of Drp1 and Mfn2. To confirm these findings, similar results were found in *in vitro study* using HK-2 cells. It indicated that VDR has a regulative effect on mitochondrial fission via inhibiting Drp1 expression and activating Mfn2 expression.

Our findings revealed that activated VDR regulated MAMs integrity and mitophagy under high glucose surroundings. VDR overexpressed plasmid and paricalcitol increased the expression level of Mfn2, restored MAMs integrity and activated mitophagy. Mfn2 was an outer mitochondrial membrane protein, previous studies mainly focused on its regulatory effect for mitochondrial fusion [50]. Recent research indicated that Mfn2 was a vital regulator of ER-mitochondria connection. Our team's latest research showed that inhibition of Mfn2 expression could abolish the MAMs integrity, and induce tubular cell apoptosis in renal tubular cell under cisplatin stimulation [52]. In this study, we found that treatment with VDR agonist calcitriol could regulate the expression of Drp1 and Mfn2 but had no effect on the expression of Mfn1 and Fis1. Besides, CO-IP analysis confirmed that VDR could directly bind and interact with Mfn2. Conversely, VDR could not bind and interact with Mfn1, Drp1 or Fis1. In order to verify the relationship among VDR, Mfn2, MAMs and mitophagy. VDR plasmid, autophagy inhibitor 3-MA, and Mfn2 siRNA were used. We found that VDR overexpressed plasmid could activate mitophagy and increase Mfn2 expression. Conversely, 3-MA treatment had no effect on the expression of VDR. On the other hand, Mfn2 siRNA treatment could partially restrain mitophagy, but has no effect on VDR expression. It demostrated that VDR was an upstream regulator of Mfn2. More critically, we found that HG/TGF-β-induced disruption of MAMs integrity in HK-2 cells was aggravated by Mfn2 siRNA, whereas the MAMs integrity and Mfn2 expression were not affected by mitophagy inhibitor, 3-MA, these results further indicated that Mfn2/MAMs was an upstream regulator of mitophagy.

SERCA2 was an integral ER channel that pumped Ca^{2+} from the cytosol to the ER lumen. It was broadly expressed in renal tubular epithelial cell. In order to identify other ER-localized factors that modulate mitochondria-ER contact. We selected SERCA2 for further analysis. We found that the expression of SERCA2 was significantly decreased under diabetic condition both in vivo and in vitro. While treatment with VDR agonist calcitriol or VDR overexpressed plasmid could increase the expression of SERCA2. In addition, the colocalization expression of Mfn2 and SERCA2 was significantly increased after paricalcitol or VDR plasmid therapy. Furthermore, CO-IP analysis showed that Mfn2 could directly bind and interact with Mfn2. Based on some latest research reports [31], we believed that the interaction between mitochondria-localized Mfn2 and ER-localized SERCA2 could regulate MAMs integrity. The distance between mitochondria and ER that were too wide (more than 50 nm) or too close (less than 5 nm) could result in MAMs dysfunction [53]. Mitochondria-ER contact promoted Ca^{2+} flux movement from ER to mitochondria, which was an essential process for the activation of some vital enzymes of the Krebs cycle to modulate mitochondrial ATP production [54]. In our study, we found that the Ca^{2+} levels in mitochondria was significantly decreased in HK-2 cells under HG/TGF-β condition, this might be a result of MAM integrity disruption and the decreased Ca^{2+} flux from ER to mitochondria. In addition, we found a decline in the levels of intracellular ATP and mitochondrial respiratory complex V (ATP synthase) activity in HK-2 cells under HG/TGF-β stimulation, while treatment with paricalcitol and VDR plasmid could partialy recover mitochondrial function. These results demonstrate a direct connection among MAMs integrity, mitochondria Ca^{2+} homeostasis and ATP production.

In brief, we found that VDR was smally expressed in mitochondria of HK-2 cells, and VDR had widespread regulating effects on mitochondrial function (e.g. mitochondrial fission, mitophagy, mitochondrial ROS, mitochondrial calcium homeostasis and MAMs integrity). However, there might be complex cross-regulation mechanisms among these aspects. And more detailed molecular regulatory mechanisms of VDR on mitochondrial dysfunction was need further exploration. Another problem was that, whether the protective effect of VDR an mitochondrial damage was relying on mitochondrial VDR or nuclear VDR. Traditional wisdom hold that VDR was a nuclear transcription regulatory factor, activated nuclear VDR could regulate various gene transcription. We believed that both mitochondrial VDR and nuclear VDR were involved in the regulation of mitochondrial function. Our team's further research will focus on the transcription regulation of nuclear VDR on the expression Drp1, Mfn2, PINK1. Moreover, the relationship between mitochondrial localized VDR and mitochondrial regulatory proteins will be further studied. Though our research had got certain results, there was also some deficiency. Firstly, we did not analysis the expression of key parameters (e.g. VDR, Mfn2) in the renal biopsy samples of DN patients. Second, we have tried to isolate of MAMs from renal tissues and HK-2 cells, but it was failed, and we could not quantitative analysis the expression levels of some parameters (e.g. FUNDC1) in MAMs. We only used ER-blue/Mitotracker double staining and TEM detection to observe MAMs integrity. Third, VDR overexpression plasmid and Mfn2 siRNA were used in this study, whereas VDR transgenic mice or Mfn2 knockout mice are needed in our future research.

5. Conclusion

Collectively, our findings showed that activation of VDR could contribute to restore mitochondrial function in renal tubular epithelial cell under DN condition(Fig. 9). VDR could restore mitophagy, inhibit mitochondrial fission, increase the levels of MMP and mitochondrial ATP production, restrain mitochondrial ROS, and restore MAMs integrity via modulation the expression of various factors. It indicated that regulation of VDR on mitochondrial function could present a novel therapeutic strategy for diabetic renal tubulointerstitial injury.

Compliance with ethical standards

None of the authors is in any condition that may represent a potential conflict of interest.

Data availability and ethics committee

The data used to support the findings of this study are available from the first author and corresponding author upon request. An electronic laboratory notebook by a specific platform was not used for data collection. The experiments was carried out according to the Ethics Review Committee of The Third Xiangya Hospital, Central South University.

CRediT authorship contribution statement

Hong Chen: Writing – original draft, Investigation, Formal analysis, Data curation. **Hao Zhang:** Writing – review & editing, Supervision, Methodology. **Ai-mei Li:** Writing – review & editing, Methodology, Data curation. **Yu-ting Liu:** Software, Investigation, Formal analysis, Data curation. **Yan Liu:** Writing – review & editing, Software, Formal analysis. **Wei Zhang:** Methodology, Formal analysis. **Cheng Yang:** Investigation, Formal analysis, Data curation. **Na Song:** Investigation, Data

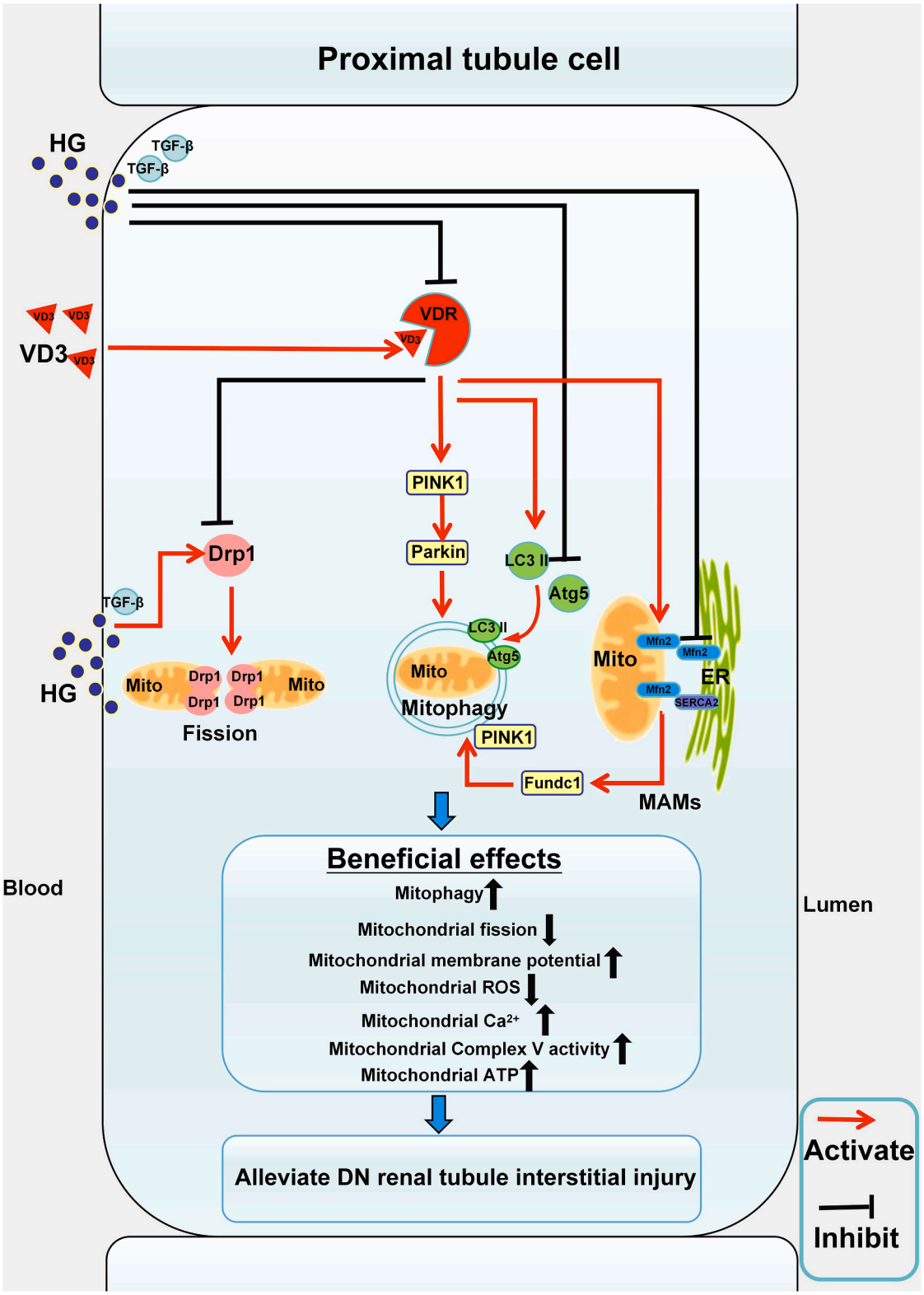

Fig. 9. A regulatory effects summary of VDR on mitochondrial function in renal tubular cell under diabetic condition.
HG stimulation significantly inhibited the expression of VDR, Mfn2, SERCA2 and mitophagy related factors (e.g. PINK1, Atg5, LC3II), but increased the expression of mitochondrial fission related factors (e.g. Drp1, Fis1). Down-regulated Mfn2 and SERCA2 could abolish the MAMs integrity and further inhibited mitophagy. Activated VDR could contribute to restore mitophagy via up-regulating of the expression of PINK1-Parkin, inhibit mitochondrial fission via down-regulating of the expression of Drp1, and restore MAMs integrity via modulation of the expression of Mfn2, SERCA2. While VDR-Mfn2-MAMs-Fundc1 pathway also could activate mitophagy. It indicated that regulation of VDR on mitochondrial function could present a new therapeutic strategy for diabetic renal tubulointerstitial injury. (For interpretation of the references to color in this figure legend, the reader is referred to the Web version of this article.)

curation, Conceptualization. **Ming Zhan:** Supervision, Methodology, Formal analysis. **Shikun Yang:** Writing – review & editing, Writing – original draft, Supervision, Methodology, Funding acquisition, Formal analysis, Conceptualization.

Declaration of competing interest

The authors report no conflicts of interest. The authors are responsible for the content and writing of the paper.

Data availability

Data will be made available on request.

Acknowledgments

This study was supported by the Hunan Provincial Clinical Medical Technology Innovation Guide Project (2020SK53601). Natural Science Foundation of Hunan Provincial (2018JJ3785, 2021JJ40925, 2022JJ70154). Natural Science Foundation of Changsha (kq2202419). National Natural Science Foundation of China (82000696). Hunan Provincial Health Commission scientific research project (202103050178)

Abbreviations Used

3- MA	3-Methyladenine
Alb	albumin
BUN	blood urea nitrogen
BSA	bovine serum albumin
Col-1	collagen type I
CO-IP	co-immunoprecipitation
DAB	diaminobenzidine
DsbA-L	disulfide-bond A oxidoreductase-like protein
DM	diabetes mellitus
DN	diabetic nephropathy
Drp1	dynamin-related protein 1
ESRD	end stage renal disease
ER	endoplasmic reticulum
FN	fibronectin
Fis1	mitochondrial fission 1 protein
HG	high glucose
H&E	hematoxylin-eosin
HK-2 cells	human proximal tubular epithelial cells line
IF	immunofluorescence
IHC	immunohistochemistry
Mfn1	mitofusin 1
Mfn2	mitofusin 2
MMP	mitochondrial membrane potential
MAMs	mitochondria-associated ER membranes
PAS	periodic acid-schiff
PACS-2	phosphofurin acidic cluster sorting protein 2
PBS	phosphate buffer solution
PBST	phosphate buffer solution tween
PTP	permeability transition pore
ROS	reactive oxygen species
siRNA	small interfering RNA
STZ	streptozotocin
Scr	serum creatinine
SD	standard deviation
SERCA2	Sarcoendoplasmic reticulum Ca^{2+} ATPase 2
TGF-β	Transforming growth factor beta
TEM	transmission Electron Microscopy
VDR	Vitamin D receptor

References

[1] J.E. Shaw, R.A. Sicree, P.Z. Zimmet, Global estimates of the prevalence of diabetes for 2010 and 2030, Diabetes Res. Clin. Pract. 87 (2010) 4–14.
[2] R.E. Gilbert, Proximal tubulopathy: Prime mover and key therapeutic target in diabetic kidney disease, Diabetes 66 (2017) 791–800.
[3] L. Zeni, A.G.W. Norden, G. Cancarini, R.J. Unwin, A more tubulocentric view of diabetic kidney disease, J. Nephrol. 30 (2017) 701–717.
[4] J.M. Forbes, D.R. Thorburn, Mitochondrial dysfunction in diabetic kidney disease, Nat. Rev. Nephrol. 14 (2018) 291–312.
[5] S. Yang, A. Li, J. Wang, J. Liu, Y. Han, W. Zhang, Y.C. Li, H. Zhang, Vitamin D receptor: a novel therapeutic target for kidney diseases, Curr. Med. Chem. 25 (2018) 3256–3271.
[6] C. Carlberg, Genomic signaling of vitamin D, Steroids 198 (2023) 109271.
[7] F. Silvagno, E. De Vivo, A. Attanasio, V. Gallo, G. Mazzucco, G. Pescarmona, Mitochondrial localization of vitamin D receptor in human platelets and differentiated megakaryocytes, PLoS One 5 (2010) e8670.
[8] C. Ricca, A. Aillon, L. Bergandi, D. Alotto, C. Castagnoli, F. Silvagno, Vitamin D receptor is necessary for mitochondrial function and cell health, Int. J. Mol. Sci. 19 (6) (2018) 1672.
[9] Y. Yin, Z. Yu, M. Xia, X. Luo, X. Lu, W. Ling, Vitamin D attenuates high fat diet-induced hepatic steatosis in rats by modulating lipid metabolism, Eur. J. Clin. Invest. 42 (2012) 1189–1196.
[10] M. El-Sherbiny, M. Eldosoky, M. El-Shafey, G. Othman, H.A. Elkattawy, T. Bedir, N. M. Elsherbiny, Vitamin D nanoemulsion enhances hepatoprotective effect of conventional vitamin D in rats fed with a high-fat diet, Chem. Biol. Interact. 288 (2018) 65–75.
[11] Z.S. Wang, F. Xiong, X.H. Xie, D. Chen, J.H. Pan, L. Cheng, Astragaloside IV attenuates proteinuria in streptozotocin-induced diabetic nephropathy via the inhibition of endoplasmic reticulum stress, BMC Nephrol. 16 (2015) 44.
[12] T.W. Tervaert, A.L. Mooyaart, K. Amann, A.H. Cohen, H.T. Cook, C. B. Drachenberg, F. Ferrario, A.B. Fogo, M. Haas, E. de Heer, K. Joh, L.H. Noël, J. Radhakrishnan, S.V. Seshan, I.M. Bajema, J.A. Bruijn, Pathologic classification of diabetic nephropathy, J. Am. Soc. Nephrol. 21 (2010) 556–563.
[13] Y.C. Han, S.Q. Tang, Y.T. Liu, A.M. Li, M. Zhan, M. Yang, N. Song, W. Zhang, X. Q. Wu, C.H. Peng, H. Zhang, SK. Yang, AMPK agonist alleviate renal tubulointerstitial fibrosis via activating mitophagy in high fat and streptozotocin induced diabetic mice, Cell Death Dis. 12 (2021) 925.
[14] X. Mou, D.Y. Zhou, D. Zhou, K. Liu, L.J. Chen, W.H. Liu, A bioinformatics and network pharmacology approach to the mechanisms of action of Shenxiao decoction for the treatment of diabetic nephropathy, Phytomedicine 69 (2020) 153192.
[15] S. Tang, X. Wu, Q. Dai, Z. Li, S. Yang, Y. Liu, B. Yi, J. Wang, Q. Liao, W. Zhang, H. Zhang, Vitamin D receptor attenuate ischemia-reperfusion kidney injury via inhibiting ATF4, Cell Death Dis. 9 (2023) 158.
[16] N. Liu, R. Lei, M.M. Tang, W. Cheng, M. Luo, Q. Xu, S.B. Duan, Autophagy is activated to protect renal tubular epithelial cells against iodinated contrast media-induced cytotoxicity, Mol. Med. Rep. 16 (2017) 8277–8282.
[17] B. Dalby, S. Cates, A. Harris, E.C. Ohki, M.L. Tilkins, P.J. Price, V.C. Ciccarone, Advanced transfection with Lipofectamine 2000 reagent: primary neurons, siRNA, and high-throughput applications, Methods 33 (2004) 95–103.
[18] N.R. Madamanchi, M.S. Runge, Western blotting, Methods Mol. Med. 51 (2001) 245–256.
[19] J.S. Lin, E.M. Lai, Protein-protein interactions: Co-immunoprecipitation, Methods Mol. Biol. 1615 (2017) 211–219.
[20] J.S. Aaron, A.B. Taylor, T.L. Chew, Image co-localization - co-occurrence versus correlation, J. Cell Sci. 131 (2018).
[21] S.W. Paddock, K.W. Eliceiri, Laser scanning confocal microscopy: history, applications, and related optical sectioning techniques, Methods Mol. Biol. 1075 (2014) 9–47.
[22] P. Tizro, C. Choi, N. Khanlou, Sample preparation for transmission electron microscopy, Methods Mol. Biol. 1897 (2019) 417–424.
[23] E. Tubbs, S. Chanon, M. Robert, N. Bendridi, G. Bidaux, M.A. Chauvin, J. Ji-Cao, C. Durand, D. Gauvrit-Ramette, H. Vidal, E. Lefai, J. Rieusset, Disruption of mitochondria-associated endoplasmic reticulum membrane (MAM) integrity contributes to muscle insulin resistance in mice and humans, Diabetes 67 (2018) 636–650.
[24] Y. Tao, J. Han, W. Liu, L. An, W. Hu, N. Wang, Y. Yu, MUC1 promotes mesangial cell proliferation and kidney fibrosis in diabetic nephropathy through activating STAT and β-catenin signal pathway, DNA Cell Biol. 40 (2021) 1308–1316.
[25] C.Y. Chung, M.R. Duchen, A plate reader-based measurement of the cellular ROS production using dihydroethidium and MitoSOX, Methods Mol. Biol. 2497 (2022) 333–337.
[26] N.A. Marcondes, S.R. Terra, C.S. Lasta, N.R.C. Hlavac, M.L. Dalmolin, L.A. Lacerda, G.A.M. Faulhaber, F.H.D. González, Comparison of JC-1 and MitoTracker probes for mitochondrial viability assessment in stored canine platelet concentrates: a flow cytometry study, Cytometry 95 (2019) 214–218.
[27] Y. Li, H.Y. Li, J. Shao, L. Zhu, T.H. Xie, J. Cai, W. Wang, M.X. Cai, Z.L. Wang, Y. Yao, T.T. Wei, GRP75 modulates endoplasmic reticulum-mitochondria coupling and accelerates Ca(2+)-dependent endothelial cell apoptosis in diabetic retinopathy, Biomolecules 12 (12) (2022) 1778.
[28] A.E. Frazier, A.E. Vincent, D.M. Turnbull, D.R. Thorburn, R.W. Taylor, Assessment of mitochondrial respiratory chain enzymes in cells and tissues, Methods Cell Biol. 155 (2020) 121–156.
[29] B. Sheng, K. Gong, Y. Niu, L. Liu, Y. Yan, G. Lu, L. Zhang, M. Hu, N. Zhao, X. Zhang, P. Tang, Y. Gong, Inhibition of gamma-secretase activity reduces Abeta production,

reduces oxidative stress, increases mitochondrial activity and leads to reduced vulnerability to apoptosis: implications for the treatment of Alzheimer's disease, Free Radic. Biol. Med. 46 (2009) 1362–1375.
[30] P.C. Liao, C. Bergamini, R. Fato, L.A. Pon, F. Pallotti, Isolation of mitochondria from cells and tissues, Methods Cell Biol. 155 (2020) 3–31.
[31] J.F. Yang, X. Xing, L. Luo, X.W. Zhou, J.X. Feng, K.B. Huang, H. Liu, S. Jin, Y. N. Liu, S.H. Zhang, Y.H. Pan, B. Yu, J.Y. Yang, Y.L. Cao, Y. Cao, C.Y. Yang, Y. Wang, Y. Zhang, J. Li, X. Xia, T. Kang, R.H. Xu, P. Lan, J.H. Luo, H. Han, F. Bai, S. Gao, Mitochondria-ER contact mediated by MFN2-SERCA2 interaction supports CD8(+) T cell metabolic fitness and function in tumors, Sci Immunol 8 (2023) eabq2424.
[32] M. Zhan, I. Usman, J. Yu, L. Ruan, X. Bian, J. Yang, S. Yang, L. Sun, Y.S. Kanwar, Perturbations in mitochondrial dynamics by p66Shc lead to renal tubular oxidative injury in human diabetic nephropathy, Clin. Sci. (Lond.) 132 (2018) 1297–1314.
[33] Y.S. Kanwar, L. Sun, P. Xie, F.Y. Liu, S. Chen, A glimpse of various pathogenetic mechanisms of diabetic nephropathy, Annu. Rev. Pathol. 6 (2011) 395–423.
[34] S.K. Yang, A.M. Li, Y.C. Han, C.H. Peng, N. Song, M. Yang, M. Zhan, L.F. Zeng, P. A. Song, W. Zhang, S.Q. Tang, H. Zhang, Mitochondria-targeted peptide SS31 attenuates renal tubulointerstitial injury via inhibiting mitochondrial fission in diabetic mice, Oxid. Med. Cell. Longev. 2019 (2019) 2346580.
[35] J. Dan Dunn, L.A. Alvarez, X. Zhang, T. Soldati, Reactive oxygen species and mitochondria: a nexus of cellular homeostasis, Redox Biol. 6 (2015) 472–485.
[36] L. Hu, H. Wang, L. Huang, Y. Zhao, J. Wang, The protective roles of ROS-mediated mitophagy on (125)I seeds radiation induced cell death in HCT116 cells, Oxid. Med. Cell. Longev. (2016) 9460462, 2016.
[37] S. Missiroli, S. Patergnani, N. Caroccia, G. Pedriali, M. Perrone, M. Previati, M. R. Wieckowski, C. Giorgi, Mitochondria-associated membranes (MAMs) and inflammation, Cell Death Dis. 9 (2018) 329.
[38] M. Xue, T. Fang, H. Sun, Y. Cheng, T. Li, C. Xu, C. Tang, X. Liu, B. Sun, L. Chen, PACS-2 attenuates diabetic kidney disease via the enhancement of mitochondria-associated endoplasmic reticulum membrane formation, Cell Death Dis. 12 (2021) 1107.
[39] M. Yang, Q. Zhang, S. Luo, Y. Han, H. Zhao, N. Jiang, Y. Liu, L. Li, C. Li, C. Liu, L. He, X. Zhu, L. Sun, DsbA-L alleviates tubular injury in diabetic nephropathy by activating mitophagy through maintenance of MAM integrity, Clin. Sci. (Lond.) 137 (2023) 931–945.
[40] X. Wei, Z. Lu, L. Li, Y. Hu, F. Sun, Y. Jiang, H. Ma, H. Zheng, G. Yang, D. Liu, P. Gao, Z. Zhu, Activation of TRPV1 channel antagonizes diabetic nephropathy through inhibiting endoplasmic reticulum-mitochondria contact in podocytes, Metabolism 105 (2020) 154182.
[41] M. Hamasaki, N. Furuta, A. Matsuda, A. Nezu, A. Yamamoto, N. Fujita, H. Oomori, T. Noda, T. Haraguchi, Y. Hiraoka, A. Amano, T. Yoshimori, Autophagosomes form at ER-mitochondria contact sites, Nature 495 (2013) 389–393.
[42] L. Liu, D. Feng, G. Chen, M. Chen, Q. Zheng, P. Song, Q. Ma, C. Zhu, R. Wang, W. Qi, L. Huang, P. Xue, B. Li, X. Wang, H. Jin, J. Wang, F. Yang, P. Liu, Y. Zhu, S. Sui, Q. Chen, Mitochondrial outer-membrane protein FUNDC1 mediates hypoxia-induced mitophagy in mammalian cells, Nat. Cell Biol. 14 (2012) 177–185.
[43] S. Wu, Q. Lu, Q. Wang, Y. Ding, Z. Ma, X. Mao, K. Huang, Z. Xie, M.H. Zou, Binding of FUN14 domain containing 1 with inositol 1,4,5-trisphosphate receptor in mitochondria-associated endoplasmic reticulum membranes maintains mitochondrial dynamics and function in hearts in vivo, Circulation 136 (2017) 2248–2266.
[44] W. Wu, W. Li, H. Chen, L. Jiang, R. Zhu, D. Feng, FUNDC1 is a novel mitochondrial-associated-membrane (MAM) protein required for hypoxia-induced mitochondrial fission and mitophagy, Autophagy 12 (2016) 1675–1676.
[45] L.A. Plum, H.F. DeLuca, Vitamin D, disease and therapeutic opportunities, Nat. Rev. Drug Discov. 9 (2010) 941–955.
[46] Z. Hu, H. Zhang, B. Yi, S. Yang, J. Liu, J. Hu, J. Wang, K. Cao, W. Zhang, VDR activation attenuate cisplatin induced AKI by inhibiting ferroptosis, Cell Death Dis. 11 (2020) 73.
[47] S. Jiang, H. Zhang, X. Li, B. Yi, L. Huang, Z. Hu, A. Li, J. Du, Y. Li, W. Zhang, Vitamin D/VDR attenuate cisplatin-induced AKI by down-regulating NLRP3/Caspase-1/GSDMD pyroptosis pathway, J. Steroid Biochem. Mol. Biol. 206 (2021) 105789.
[48] F. Silvagno, M. Consiglio, V. Foglizzo, M. Destefanis, G. Pescarmona, Mitochondrial translocation of vitamin D receptor is mediated by the permeability transition pore in human keratinocyte cell line, PLoS One 8 (2013) e54716.
[49] M.J. Haas, M. Jafri, K.R. Wehmeier, L.M. Onstead-Haas, A.D. Mooradian, Inhibition of endoplasmic reticulum stress and oxidative stress by vitamin D in endothelial cells, Free Radic. Biol. Med. 99 (2016) 1–10.
[50] M. Zhan, C. Brooks, F. Liu, L. Sun, Z. Dong, Mitochondrial dynamics: regulatory mechanisms and emerging role in renal pathophysiology, Kidney Int. 83 (2013) 568–581.
[51] M. Zhan, I.M. Usman, L. Sun, Y.S. Kanwar, Disruption of renal tubular mitochondrial quality control by Myo-inositol oxygenase in diabetic kidney disease, J. Am. Soc. Nephrol. 26 (2015) 1304–1321.
[52] Y.T. Liu, H. Zhang, S.B. Duan, J.W. Wang, H. Chen, M. Zhan, W. Zhang, A.M. Li, Y. Liu, S.K. Yang, Mitofusin2 Ameliorated Endoplasmic Reticulum Stress and Mitochondrial Reactive Oxygen Species through Maintaining Mitochondria-Associated Endoplasmic Reticulum Membrane Integrity in Cisplatin-Induced Acute Kidney Injury, Antioxid Redox Signal, 2023. Online ahead of print.
[53] M. Giacomello, L. Pellegrini, The coming of age of the mitochondria-ER contact: a matter of thickness, Cell Death Differ. 23 (2016) 1417–1427.
[54] L.S. Jouaville, P. Pinton, C. Bastianutto, G.A. Rutter, R. Rizzuto, Regulation of mitochondrial ATP synthesis by calcium: evidence for a long-term metabolic priming, Proc. Natl. Acad. Sci. U.S.A. 96 (1999) 13807–13812.